# Small mammal tooth enamel carbon isotope record of C4 grasses in late Neogene China

Arppe, Laura

2015-10

Arppe , L , Kaakinen , A , Passey , B , Zhang , Z & Fortelius , M 2015 , ' Small mammal tooth enamel carbon isotope record of C4 grasses in late Neogene China ' , Global and Planetary Change , vol. 133 , pp. 288-297 . https://doi.org/10.1016/j.gloplacha.2015.09.003

http://hdl.handle.net/10138/233850
https://doi.org/10.1016/j.gloplacha.2015.09.003

# Small mammal tooth enamel carbon isotope record of $C_4$ grasses in late Neogene China

Laura Arppe[a,*], Anu Kaakinen[b], Benjamin H. Passey[c], Zhaoqun Zhang[d], Mikael Fortelius[b]

[a]Finnish Museum of Natural History, University of Helsinki, P.O.Box 64, 00014, Helsinki, Finland

[b]Department of Geosciences and Geography, University of Helsinki, P.O.Box 64, 00014, Helsinki Finland

[c]Department of Earth and Planetary Sciences, Johns Hopkins University, Baltimore, MD 21218, USA

[d] Key Laboratory of Vertebrate Evolution and Human Origin of Chinese Academy of Sciences, Institute of Vertebrate Paleontology and Paleoanthropology, Chinese Academy of Sciences, Beijing 100044, China

* Corresponding author. E-mail address: laura.arppe@helsinki.fi (Laura Arppe)

*Post-print version. Published in Global and Planetary Change. 2015;133:288-297. Available from, DOI: 10.1016/j.gloplacha.2015.09.003*

## Abstract

The spatiotemporal pattern of the late Cenozoic spread of $C_4$ vegetation is an important indicator of environmental change that is intertwined with the uplift of the Himalaya and Tibetan Plateau, and the development of the East Asian monsoons. To explore the spread of $C_4$ vegetation in China and shed new light on regional climatic evolution, we measured $\delta^{13}C$ values of more than 200 small mammal teeth (primarily rodents and lagomorphs) using a laser ablation isotope ratio mass spectrometry approach. Small mammals are highly sensitive indicators of their environment because they have limited spatial ranges and because they have minimal time-averaging of carbon isotope signatures of dietary components. The specimens originate from four classic Late Miocene fossil localities, Lufeng, Yuanmou, Lingtai, and Ertemte, along a southwest-northeast transect from Yunnan Province to Inner Mongolia. In Yunnan (Lufeng, Yuanmou) and on the Loess Plateau (Lingtai), the small mammal $\delta^{13}C$ values record nearly pure $C_3$ ecosystems, and mixed but $C_3$-based ecosystems, respectively, in agreement with previous studies based on carbon isotopes of large herbivores and soil carbonates. In Inner Mongolia, the micromammalian tooth enamel $\delta^{13}C$ record picks up the presence of $C_4$ vegetation where large mammal samples do not, indicating

a mixed yet $C_3$-dominated ecosystem at ~6 Ma. As a whole, the results support a scenario of northward increasing $C_4$ grass abundance in a pattern that mirrors northward decreasing precipitation of the summer monsoon system. The results highlight differences between large and small mammals as indicators of $C_4$ vegetation in ancient ecosystems, particularly the ability of small mammal $\delta^{13}C$ values to detect the presence of minor components of the vegetation structure.

Keywords: $C_4$ vegetation, carbon isotopes, laser ablation, tooth enamel, rodent, East Asian Monsoon

# 1. Introduction

One of the most striking ecological transformations of the Cenozoic was the global emergence and expansion of $C_4$ grasses during the late Miocene and Pliocene, and the attendant transformation of many lineages of mammalian herbivores, with decline of forest-dwelling browsers and success of grazers of the open plains (Cerling et al., 1997; Janis et al., 2000, 2004; see Strömberg 2011 for a review). These changes are iconic examples of the overall trend of cooling and aridification that occurred since the Middle Miocene Climatic Optimum ca. 15 Ma ago. Yet, the global signal includes considerable temporal and regional variation, with some regions changing faster than others or even temporarily reversing the direction of change. In the Eurasian realm, for example, precipitation increased during the late Late Miocene in northern China while the Mediterranean experienced arid conditions (Fortelius et al., 2002; Eronen et al., 2010; Fortelius et al., 2014). Aridification was, in turn, more profound and occurred earlier in North America than in Europe (Eronen et al., 2012). In Asia, one of the main factors responsible for this heterogeneity is the regional development of monsoonal climate systems (Wang et al., 2005; Molnar et al., 2010; Tang et al., 2015).

The East Asian Monsoon is the most important monsoon system of the late Neogene. This system can be traced back to the early Cenozoic (Sun and Wang, 2005) and although considerable uncertainty remains, there is evidence from multiple proxies that a marked strengthening of the system occurred in the late Miocene (An et al., 2001; Molnar et al., 2010; Tang, 2013). Since the fundamental characteristic of a monsoon system is seasonal fluctuation between two opposing states, e.g., of precipitation and dominant wind direction (Ramage, 1971; Webster et al., 1998), a strengthened monsoon almost inevitably means strengthened seasonality. Seasonality of rainfall and temperature, in conjunction with mean values of those parameters, is the dominant control on the basic nature of prevailing ecosystems, for example, evergreen forest, deciduous forest, savanna, or grassland (e.g. Breckle, 2002).

One of the most intensely studied phenomena that is often placed in a context of monsoon history is the expansion of grasses using $C_4$ photosynthesis, the so-called $C_4$ grasses, which are favored in regions with warm growing seasons, and in conditions of reduced atmospheric $CO_2$ concentration (Ehleringer and Björkman, 1977; Ehleringer et al., 1997). The rise of $C_4$ grasses dates back to the early Oligocene (but see Vicentini et al., 2008) with rare evidence of occurrence from the Oligocene to middle Miocene (Strömberg, 2005; Tipple and Pagani, 2007; Urban et al., 2010). Today $C_4$ grasses dominate mid- to low-latitude grasslands in warm-temperate, subtropical and tropical regions, and make up ca. 20-30% of terrestrial primary production (Lloyd and Farquhar, 1994; Ehleringer et al., 1997; Fung et al., 1997; Still et al., 2003).

A dramatic increase in global $C_4$ biomass took place during the late Miocene, with a clear pattern of expansion earlier at lower latitudes and later in higher latitudes (Cerling et al 1997; Ségalen et al. 2007; Passey et al. 2009). In many regions, the emergence and expansion of $C_4$ grasses appears to have followed a two-stage pattern: a late Miocene appearance and a post-Miocene growth to dominance (e.g. Fox and Koch 2004; Ségalen et al., 2007; Martin et al. 2008; Strömberg and McInerney 2011; Biasatti et al. 2012; Fox et al., 2012). $C_4$ grasses became a significant part of herbivore diets between 9.9 and 6.5 Ma in Eastern Africa (3°S-5°N), 7 and 3 Ma in Central Africa (~16-22 °S), and 5 and 3 Ma in Southern Africa (24-25°S), but ecosystem-level open $C_4$ grasslands were established only in the Pleistocene (Cerling et al., 1997; Ségalen et al. 2007; Uno et al., 2011). In Argentina, $C_4$ plants are present in the ecosystem already at 9 Ma, and the main $C_4$ expansion took place 8-5 Ma (McFadden et al., 1996; Hynek et al., 2012). In the Great Plains of North America, soil carbonate $\delta^{13}C$ records (Fox and Koch, 2003, 2004; Fox et al., 2012) indicate a presence of $C_4$ grass throughout Miocene with increased $C_4$ abundance after 6 Ma, while herbivore diets below 37°N show a significant $C_4$ component only after 8-6 Ma (Cerling et al., 1997; Passey et al., 2002). In South Asia, proxy records from the Siwaliks of Pakistan (Quade et al., 1989; 1992; Quade and Cerling, 1995; Cerling et al., 1997; Behrensmeyer et al., 2007; Kimura et al., 2013), India (Sanyal et al., 2004; Singh et al., 2011; 2013) and Nepal (Quade et al., 1995) show the change from $C_3$ to $C_4$ biomass taking place 8-4.5 Ma. Notwithstanding claims of up to 60% $C_4$ grass in the early Oligocene (Urban et al., 2010), $C_4$ grasses have not established a significant presence in western Europe or the eastern Mediterranean region during the past 20 Myr (Cerling et al., 1997). Isotope records from China indicate a $C_4$ component in the landscape from ca. 8-7 Ma, and subsequent expansion during Pliocene to Pleistocene times (Gaboardi et al., 2005; Zhang et al., 2009; Passey et al., 2009, Biasatti et al. 2012).

As of yet, the mechanisms driving the spread of $C_4$ grasslands are not well understood and are actively debated, but the near-synchronous expansion of $C_4$ grasslands suggests a combination of a global driving mechanism modified by region-specific conditions. The list of possible factors includes the long-term evolution of atmospheric partial pressure of $CO_2$ (e.g. Cerling et al., 1997; Zhang et al., 2009; Singh et al., 2011), tectonics (Quade et al., 1989), temperature, seasonality and aridity (Pagani et al., 1999), fire

frequency (Keeley and Rundel, 2005; Scheiter et al., 2012) and, in the specific case of eastern Asia, the East Asian monsoon system (Quade et al., 1989; Quade et al., 1995; Passey et al., 2009).

The history of the global spread of $C_4$ biomass is known from the distinct isotopic signature of $C_4$ plants in the fossil record. The carbon fixation strategy of $C_4$ plants (most tropical grasses and sedges) results in reduced fractionation of carbon isotopes between atmospheric $CO_2$ and photosynthates. $C_4$ plants typically have $\delta^{13}C$ values from -15 to 10‰, significantly higher than those of $C_3$ vegetation (all trees, most shrubs, some cool/temperate climate grasses) ranging from -35 to -22‰. This large difference in isotopic composition allows for unambiguous detection of $C_4$ plants in the ecosystem, provided existence of suitable proxy materials that record the plant carbon isotopic signatures. In addition to ancient soil carbonates (e.g. Quade et al., 1989; Quade and Cerling, 1995; Latorre et al., 1997) and phytoliths (McInerney et al., 2011; Strömberg and McInerney, 2011), the carbon isotopic composition of herbivore tooth enamel has served as a window to the distant past (Cerling et al., 1993; Wang et al., 1994; MacFadden et al., 1994; 1996; Cerling et al., 1997; Passey et al., 2002; Gaboardi et al., 2005; Wang and Deng, 2005; Passey et al., 2009; Biasatti et al., 2012; Kita et al., 2014). Offset from the $\delta^{13}C$ values of the diet by 11-14‰ (Cerling et al., 1997; Cerling and Harris, 1999; Passey et al., 2005; Podlesak et al., 2008), herbivore teeth and bones reflect the isotopic composition of the consumed vegetation.

Due to sample size requirements for $\delta^{13}C$ analysis, the use of small mammal specimens for stable isotope palaeoecological studies has been very limited, and investigations have relied primarily on thick-enameled large mammals. Yet micromammals are common in the fossil record, and make up an important component of terrestrial ecosystems, and with their generally high fecundities, high local densities and population growth rates they hold tremendous potential as sensitive and quickly responding recorders of environmental changes. Other than size-imposed restrictions, micromammalian isotopic proxy records show no disadvantage compared to larger animals (Gehler et al., 2012), and have proven useful in a number of pioneering studies (e.g. Grimes et al., 2005; Hopley et al., 2006; Yeakel et al., 2007; Hynek et al., 2012; Kimura et al., 2013). Hynek et al. (2012) recently demonstrated the value of micromammalian $\delta^{13}C$ values in Argentina, which enabled detection of the presence of $C_4$ vegetation in the ecosystem 1-2 Ma earlier than indicated by large mammal and soil carbonate $\delta^{13}C$ records. The sensitivity of small mammals as recorders of their environment is linked to their physiologies. The small mass of dietary intake leads to a greater probability of sampling end-member isotope compositions, and the relatively quick growth rate of micromammalian dental tissue (Passey et al., 2005; Podlesak et al., 2008) leads to decreased dampening and homogenization of isotope signals. Thus, the possibilities of capturing the full range of isotope values present in the environment are heightened using a sampling of many small mammal taxa. The small areal ranges of individual micromammals promotes an ‘in situ’ nature of the record, and thus affords potential for the reconstruction of landscape patchiness.

Taking advantage of laser-based methods (Sharp and Cerling, 1996; Passey and Cerling, 2006) allowing routine analyses of very small samples, we explore the potential of the rich micromammalian fossil faunas in four late Neogene localities across China, and attempt to shed new light on the evolution of climate and spread of $C_4$ vegetation in eastern Asia. The abundance of micromammalian remains allows for high sample replication (in terms of numbers of individual tooth specimens analyzed) and comprehensive, representative sampling of the herbivore small mammal community. We present a data set from more than 200 small mammal tooth specimens, and compare the micromammalian dietary record with that of large mammals, discussing the potential reasons for the observed differences and their implications for future isotope work on small mammals. Based on the new $\delta^{13}C$ data, we update our current knowledge – largely based on paleosol and large herbivore isotope proxies – on regional $C_4$ signal histories and view these histories in the larger perspective of late Neogene climatic and ecological evolution in East Asia.

## 2. Regional Setting

Fossil material was collected from four localities (Fig.1): two from northern China (Ertemte and Lingtai) and two from southern China (Lufeng and Yuanmou). The modern climate in all these areas is under the influence of seasonal alterations of the East Asian summer monsoon and the Siberian-Mongolian winter monsoon, and the sites in southern China are also strongly influenced by the Indian summer monsoon. During summer seasons, high pressure cells form over the Indian and Pacific oceans and give rise to the warm and humid winds migrating into the interior China. During winter seasons the atmospheric pressure gradient is reversed and the cold and sometimes dust-laden winds, driven by the Siberian high pressure, migrate along the northern and eastern margins of the Tibetan Plateau to South China (An et al., 1990; An, 2000).

The Ertemte site (41°54'N 114°6'E) is located 4 kilometers southeast of the town of Huade in the Inner Mongolian Autonomous district. The area belongs to the temperate grassland and steppe zone, and mean annual temperature and rainfall are 3.2 $^{o}$C and 329 mm (WordClim). Knowledge of the Ertemte fauna dates back to almost a century ago (Andersson, 1923; Schlosser, 1924), and it now is the most diverse and abundant Late Miocene mammalian fauna in China. The mammalian assemblage is composed of 66 species of both small and large mammals (Qiu Z.-D. et al., 2013), collected from a limited stratigraphic horizon within a unit of lacustrine deposits. The age of the Ertemte fauna is based on biochronology, and it is considered to be equivalent to late MN13 (corresponds approximately to late Turolian, ca. 7-5 Ma; Storch, 1987, Qiu et al., 2006). Based on Flynn et al. (1997), Ertemte can be correlated with the basal Gaozhuang formation, which is dated magnetostratigraphically to C3r (6.033–5.235 Ma; Opdyke et al., 2013), and here we use 5.5 Ma as a rough estimate of the age of the Ertemte fauna. The Ertemte assemblage represents a typical Hipparion fauna. Though not systematically reviewed since the description by Schlosser (1924), large

mammals are characterized by abundant cervids, and few bovids. Micromammals are characterized by a high diversity of insectivores and myomorph rodents, and high generic diversity of ground squirrels and lophate cricetids (Qiu Z.-D. et al., 2013). Our survey covers more than half of the Ertemte small mammal taxa.

The Lingtai fossil material (35° 03'N 107° 44'E) comes from a stratigraphic section in Leijiahe village, Lingtai county, in Gansu province in the central Loess Plateau (LP), ca 10 km east from Lingtai town. The area belongs to the warm temperate deciduous-broadleaf forest zone with annual temperature and precipitation of about 10.7 $^{o}$C and 620 mm (WordClim), respectively. The late Miocene–Pliocene strata resting on the Cretaceous basement are mainly fluvial silts and sands that reach a composite thickness of ca. 60 m, overlain by Pleistocene loess and paleosol deposits. Repeated collecting activities in Leijiahe area since 1970's have resulted in numerous superposed micromammal faunas, consisting altogether of 80 micromammal forms (Zheng and Zhang, 2001; Qiu Z.-X. et al., 2013), whereas the large mammal fossils collected at the site are sparse and fragmentary, dominated by herbivores like *Hipparion* and *Gazella* (Chen et al., 2002). Age control of the fossiliferous levels comes from magnetostratigraphy (Wei et al., 1993). The micromammalian samples in this study originate from eight different stratigraphic levels spanning 6.6 to 3.16 Ma in age. We have approximated the ages of the fossil beds using linear interpolation for upper and lower limits of fossil-bearing magnetozones.

The Lufeng fossil material (25° 18'N 102° 24'E) comes from near Shihuiba village in the Lufeng basin, located about 65 km northwest of the provincial capital, Kunming, Yunnan Province. The locality lies east of the Dianzhong Plateau, in a fault depression that has mean elevation of 1560 m. The area belongs to the temperate mountain forest and subtropical forest zone with the mean annual temperature of 15.2 $^{o}$C and rainfall of 953 mm (WorldClim)). Lufeng is renowned for the fossil hominoid *Lufengpithecus lufengensis* and for being the most fossiliferous and taxonomically diverse late Neogene locality in South China (Qiu et al., 2013). The Late Miocene exposures comprise a 20–30-m-thick succession (Dong and Qi, 2013) in which the fossil bearing sediments are massive lignites that are ca. 5–6 m thick, alternating with carbonaceous clays, silts and sands with interbedded lignites (Harrison et al., 2002). Since the discovery of hominoid materials in the late 1970's, altogether 98 mammal taxa have been uncovered from the Shihuiba Formation, including three taxa of primates, and diverse ungulate and rodent fauna. Paleomagnetic ages of ca. 4 Ma (Yin, 1994) and 6.9-6.2 Ma (Dong and Qi, 2013) have been reported for the hominoid-producing horizon. However, the paleomagnetic age estimates are considered to be too young to be concordant with the mammalian fauna (cf. Flynn and Qi, 1982; Harrison et al., 2002), which compare to the Late Miocene assemblages in Europe. Furthermore, the Lufeng rhizomyd rodents are equivalent to those at 8 Ma in Siwaliks, Pakistan (Flynn and Qi, 1982). Based on these constraints, recognizing that the age is associated with large error bars, we use

an approximation of 7.5 Ma for the fossil bed for the purposes of plotting. This is also in concert with the estimated age in Biasatti et al. (2012)

The Yuanmou Basin (25°42'N 101°52'E) in Yunnan Province is located ca 110 km northwest of Kunming, on the northern edge of the Dianzhong plateau with an average elevation of about 1100 m a.s.l. (Qiu et al., 2013). The area has mean annual temperature of 19.03 °C and of rainfall 790 mm (WorldClim) with strong seasonal variation. The Neogene deposits (Xiaohe Formation) are mainly distributed in the northwestern part of the basin and comprise more than 80-m-thick series of fluvial and lacustrine sediments containing abundant mammalian fossils. Altogether 110 mammalian species have been recovered from the Xiaohe Fm (Dong and Qi, 2013). The Yuanmou hominoid fauna is dominated by carnivores, rodents and artiodactyls (Qi et al., 2006). Qi et al. (2006) published a paleomagnetic age of ca. 7.2 – 8.1 Ma for the Xiaohe Fm. Based on micromammalian assemblages, Ni and Qiu (2002) conclude that the Yuanmou fauna is slightly older than that of Lufeng. Therefore, based these constraints we assign an estimated age of 8 Ma to the Yuanmou micromammal samples, consistent with the estimation presented in Biasatti et al. (2012).

# 3. Material and methods

The study material comprises screen washed rodent and ochotonid lagomorph teeth (n=223; Table 1, Appendix 1). The majority of sampled teeth are adult M1 molars, although a few ochotonid incisors were also analysed. All specimens belong to the collections of the Institute of Vertebrate Paleontology and Paleoanthtropology, Beijing, China. The tooth material from Ertemte (n=142) and Lingtai (n=63) is very well preserved, with yellow to light brown coloring, and clean, clear enamel surfaces. Prior to laser analysis, the teeth were washed in MilliQ water in an ultrasonic bath. The relative proportions of different taxa that were analyzed reflects the relative abundance of taxa at the localities, which are usually dominated by cricetids. The material from the Yunnan province (n=18) is less well preserved, with variable coloring from light brown to black and the enamel surfaces often partially covered by sediment. In addition, some surfaces showed remains of adhesive putty. The Yunnan material was treated with trichloroethylene solution and MilliQ water under ultrasonic agitation to remove traces of putty and sediment.

The stable isotope analyses were carried out at Johns Hopkins University using a Photon-Machines Fusions 30 watt $CO_2$ laser coupled to a custom built partially-automated extraction line following the general design of Passey and Cerling (2006). The isotope ratios of the $CO_2$ extracted from the tooth enamel were measured on a Thermo MAT 253 mass spectrometer. The analytical procedures and data reduction protocols follow those outlined in Passey and Cerling (2006). The $\delta^{13}C$ and $\delta^{18}O$ values reported for each specimen represent the mean of one to eight individual analyses. After data reduction, a correction of +0.5‰ was applied to the $\delta^{13}C$ values to account for the systematic offset observed between laser-based

$\delta^{13}C$ values and those derived from the conventional phosphoric acid method (Passey and Cerling, 2006). Estimates of the relative proportions of $C_3$ and $C_4$ plants ingested (reported as percent $C_4$) follow the approach of Passey et al. (2002), where the $\delta^{13}C$ values of $C_3$ plants, water-stressed $C_3$ plants and $C_4$ plants are calculated from temporally varying $\delta^{13}C$ values of atmospheric $CO_2$. To account for the isotopic fractionation between enamel and diet, an enrichment factor of 11.0‰ is used (c.f. Bywater-Reyes et al., 2010; Hynek et al., 2012). Whether the chosen enrichment factor is appropriate for all small bodied mammals remains untested, but recent findings of a smaller enamel-diet fractionation for wood rats (11.0‰ ±0.1; Podlesak et al., 2008) and voles (11.5‰ ±0.3; Passey et al., 2005) relative to large mammals (ca. 14‰; Cerling and Harris, 1999) add to the growing pool of evidence of smaller enrichment factors for small mammals (ca. 9-10‰ for laboratory rats and mice: DeNiro and Epstein, 1978; Ambrose and Norr, 1993; Tieszen and Fagre 1993; Jim et al. 2004) .

The $\delta^{18}O$ values obtained by laser ablation represent a mixture of oxygen from the phosphate, carbonate and hydroxide components of the hydroxyapatite. The isotopic offset between laser and conventional phosphoric acid digestion $\delta^{18}O$ values is systematic in direction but variable in magnitude, averaging –5.1‰ with a standard deviation of 1.2‰ for multiple laser-conventional comparisons reported by Passey and Cerling (2006). Due to the uncertainty of the isotopic offset, we do not attempt to reconstruct paleo-water $\delta^{18}O$ values using laser-based enamel $\delta^{18}O$ values. The rodent enamel $\delta^{18}O$ data are included in Figure 2 and in Appendix 1, but they are not interpreted nor discussed further in this paper.

A limitation of the laser ablation approach is that the laser will sample any material it impinges upon, including organic compounds on or in the tooth enamel (e.g., glues and cements used by curators, sedimentary organic carbon, and residual structural organics in the biomineral itself). Laser ablation of organic compounds in the helium-purged, oxygen-free atmosphere of the sample chamber results in pyrolization, visible as charring and production of smoke and other lingering vapors (Passey and Cerling, 2006). Any oxidation to $CO_2$ of organic carbon would be expected to lower our observed $\delta^{13}C$ values, because organic carbon typically has lower $\delta^{13}C$ values than coexisting inorganic carbon. In our study, data from all analyses associated with heavy charring and smoke production were discarded (n=21). Some analyses resulted in production of incipient char halos or slight charring of the laser pit bottom, indicating minor contamination with organic carbon. Although Passey (2007) reports no significant difference in $\delta^{13}C$ between "minor char" and “clean” analyses, we observe a small, but statistically significant difference (paired t-Test; $p<0.05$) in mean $\delta^{13}C$ values between minor char (-10.8‰ ± 1.8) and clean (-10.6‰ ± 1.9) analyses of the same tooth specimens (n=58). However, this difference is inconsequential compared to the difference in $\delta^{13}C$ between $C_3$ and $C_4$ vegetation (ca. 15‰). Thus, because our objective is differentiating between $C_3$ and $C_4$ plant consumption, we apply no correction to the minor char analyses, and include these data in the overall data set.

# 4. Results

The isotopic data are plotted in Figures 2 and 3, and summarized in Table 1. The full dataset of $\delta^{13}C$ values is reported in Appendix 1. Except for the smallest specimens where molar size limited the number of analyses to one (n=17), the reported values represent the mean of two to eight replicate analyses. The average standard deviation of sample replicates was 0.3 ± 0.3‰ (1σ) and 0.2 ± 0.3‰ for $\delta^{13}C$ and $\delta^{18}O$, respectively. Appendix 1 includes also $\delta^{13}C$ and $\delta^{18}O$ values of large herbivore enamel from Yunnan, previously presented only in a thesis (Passey, 2007).

The $\delta^{13}C$ values of tooth enamel fall between -15.6 and -3.4 ‰, with a total range of 12.2 ‰. The majority of $\delta^{13}C$ data fall below -8 ‰; only 14 specimens show less negative $\delta^{13}C$ values (Fig. 2). Specimens from Ertemte and Lingtai show significantly overlapping ranges and comparable mean values (t-Test >0.05), with $\delta^{13}C$ values from -13.1 to -4.5 ‰ and -14.9 to -3.4, respectively. The data from Yuanmou and Lufeng in the Yunnan province plot to the lower end of the total $\delta^{13}C$ range, from -15.6 to -8.9 ‰. They are statistically indistinguishable from each other, but differ significantly (t-Test $p<<0.001$) from the datasets of Lingtai and Ertemte.

The calculated proportions of $C_4$ plants (%$C_4$) in the diets of the small mammals are listed in Table 1 and illustrated in Figure 3. Apart from one murid from Lufeng with an estimate of 23% $C_4$, the Yunnan rodents show $C_3$ based diets at ~8-7 Ma. In Lingtai and Ertemte, various levels of $C_4$ intake are observed. In Lingtai, $C_4$ contribution to diet varies from 0 to 73%, with estimates of more than 30% for only 5 out of 63 specimens. The gerbil species *Pseudomeriones abbreviatus* (n=15), sampled from stratigraphic levels with ages 6.45 Ma, 5.8 Ma, 4.8 ma and 4.7 Ma, shows an increasing trend in the amount of $C_4$ grass consumed from 6.45 Ma (0%) to 4.7 Ma (up to 73%) (Appendix). At Ertemte, $C_4$ consumption ranges from 0 to 60%, and only 10 out of 142 specimens indicate more than 30% $C_4$ intake. At both Lingtai and Ertemte, all taxa reaching a $C_4$ grass contribution of ca. 50% or above belong to muroids (the families Cricetidae and Muridae). Individuals in the families Ochotonidae and Dipodidae also consumed significant (≥30%) amounts of $C_4$ vegetation.

# 5. Discussion

## 5.1 Lingtai

In Lingtai, the mean $\delta^{13}C$ values of micromammalian enamel at the sampled stratigraphic levels increase from -11.3 ‰ at 6.45-6.6 Ma to -10.0 ‰ at 3.16 Ma, but this apparent change is not statistically significant.

Due to the scarcity of large vertebrate fossil material in the late Miocene to Pliocene strata, prior $\delta^{13}C$ data on teeth and bones do not exist from Lingtai. However, the small mammal isotope data may be compared with a soil carbonate $\delta^{13}C$ record (Fig. 3b) from the same time period (Ding and Yang, 2000) taking into account a ca. 3‰ larger offset from source plants for pedogenic carbonate compared to small mammal enamel ($\Delta_{carbonate\text{-}biomass}$ ~13.5‰ at 25°C; Cerling and Quade, 1993). Prior to 4 Ma the soil carbonate data are interpreted to reflect a $C_3$ dominated ecosystem (Ding and Yang, 2000), with plant biomass $\delta^{13}C$ values of -22 to -23‰. $C_4$ plants were, however, present at Lingtai, perhaps as spatially very limited patches, as registered by the few higher small mammal enamel $\delta^{13}C$ values at 6.6, 5.8 and 4.7 Ma. The particularly high $\delta^{13}C$ value of one specimen at 4.7 Ma illustrates this patchiness, and yet again documents the increased affinity of micromammals to register end-member isotope compositions.

Even after 4 Ma, when the soil carbonate $\delta^{13}C$ values begin to rise, $C_4$ plant abundance in the landscape seems to have remained limited (Ding and Yang, 2000). A single soil carbonate peak value of -4.7‰ at 3.4 Ma corresponds to mean plant $\delta^{13}C$ values of -19‰, suggesting a maximum of ~30% $C_4$ biomass. The mean values of small mammal enamel match the soil carbonate record. For the sampling levels at 3.46 Ma, 3.35 Ma and 3.16 Ma, mean micromammal-inferred plant biomass $\delta^{13}C$ values are -21.8, -21.1, and -21.0‰, while the soil carbonate data indicate plant $\delta^{13}C$ values of -21.5, 20 and -21‰, respectively. Translated into percent $C_4$ vegetation and averaged, both records suggest ~15% contribution from $C_4$ vegetation over the 3-3.5 Ma interval, indicating a mixed, but still a clearly $C_3$ dominated ecosystem prevailed on the Loess Plateau.

## 5.2 Inner Mongolia

The micromammalian enamel $\delta^{13}C$ values from Ertemte indicate the presence of $C_4$ grasses in the local ecosystem at ~5.5 Ma. The spatial and temporal patterns of $C_4$ vegetation in Central Inner Mongolia were previously studied by Zhang et al. (2009) based on enamel $\delta^{13}C$ values of various large herbivores. They infer a first appearance of a significant $C_4$ component in the landscape in the 7.5 Ma Baogedawula locality ca 200 km NE of Ertemte (Figure 3a), where the $C_4$ component of herbivore diets ranged from 0 to 29%. There are no large herbivore data from the intervening time period from that region, but again at 3.9 Ma horses and elephantids from the Gaotege locality (G in Figure 1) were estimated to have incorporated 19 to 53% $C_4$ plants in their diets. For Ertemte (~5.5 Ma) and the nearby locality of Bilike (4.7 Ma), the large mammal enamel $\delta^{13}C$ data indicate a pure $C_3$ diet. The carbon isotopic composition of diet for the large herbivores, -27 to -24‰, is considerably lower than that inferred for the micromammals, -24.4 to -15.5‰. Making a note of possible inadequacy in number of samples (n=6), they hypothesize that the pure $C_3$ diet of large herbivores reflects a retreat of $C_4$ vegetation after an initial expansion at 7.5 Ma (inferred from the

Baogedawula area), or that the Ertemte area remained forested without any $C_4$ plants in the latest Miocene and Pliocene due to a warmer and wetter climate.

The small and large mammal $\delta^{13}C$ data are not necessarily in conflict, but may be explained by their inherent characteristics. Contrary to micromammalian isotope records, $\delta^{13}C$ values of large herbivores do not necessarily represent a strictly local vegetation signal (e.g. Zazzo et al., 2010). Differences may thus reflect larger range areas or migratory behavior of large herbivores. Also, as discussed in the Introduction, micromammalian $\delta^{13}C$ records have the potential to detect smaller abundances of $C_4$ plants in the ecosystem due to the smaller biomass consumed and shorter temporal timespan over which the signal is averaged. Thus it is possible that the proportion of $C_4$ grasses in Ertemte was small enough not to show up in large herbivore diets, suggesting low to moderate levels of $C_4$ vegetation in the landscape. According to a survey of local plants, $C_4$ grasses constitute a minor component of the present-day ecosystem in the area (Zhang et al., 2009).

## 5.3 Yunnan

The diets of the rodents from the Yunnan province are more $^{13}C$-depleted (mean -24‰) than those of small mammals from the northern and central parts of China (mean -21.4‰), and with a single exception are consistent with pure $C_3$ vegetation. This suggests a strongly $C_3$ dominated environment, in agreement with other lines of evidence. For example, based on small mammal assemblages, the paleoenvironmental context at Yuanmou and Lufeng has been interpreted as a tropical forest with scattered shrub and grasslands (Ni and Qiu, 2002; Qi et al., 2006). In a habitat-type analysis of the micromammalian communities, Ni and Qiu (2002) show that over 80% of the small mammal taxa were restricted to or preferred mesic/forested habitats, while only ~3-5% lived in bush and grasslands.

The predominantly closed, forested biomes of Yunnan are also reflected as low $\delta^{13}C$ values of large herbivore taxa (Passey, 2007; Biasatti et al., 2012). Compared to ungulates from contemporaneous fossil localities on the Loess Plateau, those at Yuanmou displayed markedly lower enamel $\delta^{13}C$ values, indicative of a diet consisting solely of $C_3$ vegetation (Passey, 2007). This agrees with the findings of Biasatti et al. (2012), who inferred nearly pure $C_3$ diets for large herbivores prior to 2-3 Ma at six localities in the Yunnan province. However, $C_4$ grasses were evidently present in the landscape, most likely in scattered patches of more open habitat. These microhabitats left an imprint on the $\delta^{13}C$ values of paleosol carbonates and large mammal enamel (Biasatti et al., 2012), and could have served as the source of the $C_4$ signal observed here for a single Lufeng murid.

## 5.4 $C_4$ expansion and climate

The spatiotemporal systematics of the spread of $C_4$ grasses is intrinsically linked to the climatic evolution of a region. Accumulating evidence from paleosol carbonate $\delta^{13}C$ values from several localities in northern China (Ding and Yang, 2000; Jiang et al., 2002; An et al., 2005; Kaakinen et al., 2006, Passey et al., 2009, Suarez et al., 2011) indicates the presence of a spatial climatic gradient defined by northward increasing $\delta^{13}C$ values and, thus, abundance of $C_4$ grasses, in the late Miocene and Pliocene (~7 to 2.7 Ma; Passey et al., 2009; Suarez et al., 2011) as a contrast to the late Pleistocene and present day spatial pattern of southward increasing abundance of $C_4$ grass on the loess Plateau.

This reversed late Miocene to Pliocene pattern finds further support from large herbivore enamel $\delta^{13}C$ records across China (Passey et al. 2009). The following is a brief summary of the large herbivore $\delta^{13}C$ records for ~8-4 Ma (the period of good spatial data coverage), with the ages in the parentheses representing the total age span of the fossil specimens at each site. The maximum $C_4$ abundance is recorded in Yushe (6.3-2 Ma), east of the Loess Plateau (see Fig. 1), where herbivore diets commonly consisted of 50% $C_4$ forage (Passey, 2007; Passey et al., 2009).To the north, Baode (7-5.5 Ma) on the northern Loess Plateau, and Baogedawula (7.5 Ma), Ertemte (5.5 Ma), Bilike (4.7 Ma) and Gaotege (3.9 Ma) in Inner Mongolia are $C_3$ dominated, but animal diets at Baode, Baogedawula and Gaotege show moderate levels of $C_4$ grass (Passey, 2007; Passey et al., 2009; Zhang et al., 2009; Kaakinen et al., 2013; Eronen et al., 2014). For the 7.5-4.7 Ma ungulates from Baode and, Baogedawula $C_4$ grasses contributed 0-30% to their diet, while the 3.9 Ma large mammal diets in Gaotege show a $C_4$ component of up to 50%. To the south of the $C_4$ maximum zone at Yushe, the late Miocene localities at Lantian (9.95-6.6 Ma) in the central Loess Plateau also indicate $C_3$ based ecosystems with little $C_4$ vegetation (Passey et al., 2009). Only 6 out of 55 ungulate individuals incorporated up to 10% of $C_4$ in their diets. Passey et al. (2009) suggest that Lantian might have been a relatively forested milieu during the late Miocene. Even further south in Yunnan, large herbivores at Yuanmou, Lufeng, Baoshan and Zhaotong (8.5-1.75 Ma, 7.5 Ma, 5 Ma - 9 ka, 4 Ma, respectively; Biasatti et al. 2012; Passey, 2007), show little to no evidence of $C_4$ grass in their diets. However, from 3 Ma $C_4$ vegetation became a significant part in the diets of herbivores in Yunnan (Biasatti et al., 2012), indicating a substantial change in regional environmental parameters taking place between 3.5-2.5 Ma. Incidentally, a contemporaneous change in climatic regime is also observed on the Loess Plateau and Inner Mongolia. In Lingtai and Lantian, the $\delta^{13}C$ sequences of pedogenic carbonate display a peak between 3.4-2.7 Ma (Ding and Yang, 2000; An et al., 2005; Kaakinen et al., 2006; Suarez et al., 2011) suggesting transient improved conditions for $C_4$ growth during that time. In Inner Mongolia moderate levels of $C_4$ grasses are still observed at 3.9 Ma in Gaotege, while presently they account for an insignificant amount of the local biomass (Zhang et al., 2009) suggesting a retreat or at least a significant reduction of $C_4$ vegetation in the area.

The micromammalian $\delta^{13}C$ data, suggesting $C_3$ based environments with some occurrence of $C_4$ grasses at both Lingtai and Ertemte, and pure $C_3$ vegetation for Yunnan, are consistent with the spatiotemporal

pattern emerging from the soil carbonate and large mammal $\delta^{13}C$ records. According to this pattern a zone of optimum $C_4$ growth was located somewhere south of Baode and the Inner Mongolian localities at 8-4 Ma, and $C_4$ abundance decreases both to the north and south of this maximum zone (Passey et al. 2009). This pattern and the environmental changes reflected in the soil carbonate records and Yunnan herbivore diets at 3.5-2.5 Ma can be explained by a conceptual model proposed by Passey et al. (2009). In this scenario, the environmental gradient maintained by the East Asian Monsoon system, characterized by $C_3$ forests in the southeast changing to $C_3 + C_4$ steppe, and finally to the increasingly arid and cool $C_3 + C_4$ biomes in the northwest, was shifted towards the north during a period of strengthened East Asian summer monsoon. A subsequent weakening of the moisture laden summer monsoons during 3.5-2.5 Ma caused a southward retreat of the forest-steppe-desert transition, moving the $C_4$ maximum steppe zone further away from the northern localities in Inner Mongolia, through the central and southern Loess Plateau localities Lingtai and Lantian. This shift might have been related to the establishment of the present state of focused summer rains with little spring, autumn and winter precipitation (Suarez et al., 2011).

## 5.5 Late Miocene immigrants to China

The hypothesis of Passey et al. (2009) assumes active operation of the summer monsoon system during late Miocene to early Pliocene in East Asia, and it finds support from several other lines of evidence pointing towards humid and warm conditions during this time (e.g. Rea et al., 1998, Ding et al., 1999; Fortelius et al., 2002; Jia et al., 2003; Ma et al,. 2005*;* Fortelius and Zhang, 2006; Wu et al., 2006; Wang et al., 2006; Kaakinen et al., 2006; Rao et al., 2008; Sun et al., 2010; Xing et al., 2012). The Late Miocene humidity of Northern China is in stark contrast to the global trend of mid-latitude drying at that time (Fortelius et al., 2002), and it seems to have created a favorable setting for the influx of immigrant herbivorous land mammals from several directions, and the later development of endemic taxa from both native and immigrant origin (Fortelius and Zhang, 2006; Mirzaie Atabaadi et al., 2013).

Similar to large mammals, rodents show a pattern of endemism and immigrations during the later late Miocene, the Baodean Land Mammal Age (Fortelius and Zhang, 2006). According to recorded occurrences in the New and Old Worlds Database of Fossil Mammals (NOW-database; dataset downloaded 13th November 2013; Fortelius, 2014), three of the 32 small mammal genera included in our analyses made their first appearance in China in the late Miocene, later than their first occurrences in the West. They are *Apodemus*, *Occitanomys* and *Pseudomeriones*, incidentally the same three genera whose members were observed to incorporate >50% $C_4$ in their dietary intake (Table 1). A fourth "high-$C_4$" cricetid, *Sinocricetus*, is endemic to East Asia. The distributions of the three "high-$C_4$" taxa at time periods 11.2-8.2 Ma and 8.2-5.3

Ma are illustrated in Figure 4, which shows that after 8.2 Ma, these genera, especially *Occitanomys* and *Apodemus*, expanded considerably in Europe and extended their distribution to the Far East. The significance of this pattern is hard to assess on its own, since the small mammal record of the earlier late Miocene is relatively sparse in China. However, a similar pattern of apparent eastwards dispersal was observed for large mammals by Mirzaie Ataabadi et al. (2013) though in this case the pattern could be anchored in dental ecometrics suggesting that the dispersal was driven by increased humidity. The eastwards dispersal of these small mammal taxa might well be part of the same continental-scale biogeographic process.

If the pattern is not an artifact of a temporal sampling bias, it is inviting to hypothesize that the onset of strong summer monsoons and the establishment of $C_4$ ecosystems likely opened new ecological opportunities for these "high-$C_4$" taxa.

# 6. Conclusions

The $\delta^{13}C$ data from Late Miocene and Pliocene small mammal teeth from China are consistent with prior Chinese soil carbonate and large mammal isotope data establishing a scenario of northward increasing $C_4$ abundance that in turn mirrors the climatic gradient set up by the East Asian monsoons. The carbon isotope data suggest an essentially pure $C_3$ environment for Yunnan around 7.5 Ma, in agreement with other lines of evidence indicating dense, forested biomes. For Lingtai, on the Loess Plateau, the small mammal $\delta^{13}C$ values indicate the presence of $C_4$ vegetation amidst a clearly $C_3$-dominant landscape between 6.6-3.16 Ma. The small mammal record from Ertemte detects the presence of a $C_4$ component where large mammal diet data indicate a pure $C_3$ environment. In Lingtai and Ertemte, 7-8% of the small mammals incorporated more than 30% $C_4$ in their diets. The results draw attention to differences in the nature of $\delta^{13}C$ records generated from small versus large mammals and suggests that small mammals are ideal for detecting the first, faint signals of $C_4$ emergence in ecosystems.

# Appendix. Supplementary data

The Appendix is an Excel-file containing the full data set of laser-generated $\delta^{13}C$ and $\delta^{18}O$ values of small mammal tooth enamel, and $\delta^{13}C$ and $\delta^{18}O$ data of large herbivore tooth enamel from Yunnan by Passey (2007) discussed in sections 5.3 and 5.4.

# Acknowledgements

We thank Prof. Qiu Zhuding from IVPP who generously provided the small mammal specimens from Lufeng, Yuanmou and Ertemte. We thank Jussi Eronen for discussions and David Fox and an anonymous reviewer for thorough and constructive reviews. Financial support from the Academy of Finland (Grant numbers 257850 and 264935 ), National Natural Science Foundation of China (41472003), Major Basic Research Projects (2012CB821904) of MST of China, and the Waldemar von Frenckell foundation is gratefully acknowledged.

# References

Ambrose, S. H. and Norr, L., 1993. Carbon isotope evidence for routing of dietary protein to bone collagen, and whole diet to bone apatite carbonate: purified diet growth experiments. In Lambert, G., Grupe, G. (Eds), Prehistoric Human Bone Archaeology at the Molecular Level. Springer-Verlag, p. 1–37.

An, Z.S., 2000. The history and variability of East Asian paleomonsoon climate. Quaternary Science Reviews 19, 171–187.

An, Z.S., Liu, T.S., Lu, Y.C., Porter, S.C., Kukla, G., Wu, X.H., Hua, Y., 1990. The long-term paleomonsoon variation recorded by the loess-paleosol sequence in central China. Quaternary International 7, 91–96.

An, Z.S., Kutzbach, J.E., Prell, W.L., Porter, S.C., 2001. Evolution of Asian monsoons and phased uplift of the Himalayan Tibetan Plateau since Late Miocene times. Nature 411, 62–66.

An, Z.H., Huang, Y.S., Liu, W.G., Guo, Z.T., Clemens, S., Li, L., Prell, W., Ning, Y.F., Cai, Y.J., Zhou, W.J., Lin, B.H., Zhang, Q.L., Cao, Y.N., Qiang, X.K., Chang, H., Wu, Z.K., 2005. Multiple expansions of $C_4$ plant biomass in East Asia since 7 Ma coupled with strengthened monsoon circulation. Geology 33, 705–708.

Andersson, J.G., 1923. Essays on the Cenozoic of Northern China. Geological Survey of China Memoir, Series A 3, 1–152

Behrensmeyer, A.K., Quade, J., Cerling, T.E., Kappelman, J., Khan, I.I., Copeland, P., Roe, L., Hicks, J., Stubblefield, P., Willis, B.J., Latorre, C., 2007. The structure and rate of late Miocene expansion of $C_4$ plants: evidence from lateral variation in stable isotopes in paleosols of the Siwalik Group, northern Pakistan. Geological Society of America Bulletin 119, 1486–1505.

Biasatti, D., Wang, Y., Gao, F., Xu, Y., Flynn, L., 2012. Paleoecologies and paleoclimates of late Cenozoic mammals from Southwest China: Evidence from stable carbon and oxygen isotopes. Journal of Asian Earth Sciences 44, 48–61.

Breckle, S.-W., 2002. Walter's vegetation of the Earth: the ecological systems of the geo-biosphere, 4th ed., Springer-Verlag, Berlin.

Bywater-Reyes, S., Carrapa, B., Clementz,M., Schoenbohm, L., 2010. Effect of late Cenozoic aridification on sedimentation in the Eastern Cordillera of northwest Argentina (Angastaco basin). Geology 38, 235–238.

Cerling, T. E., Quade, J., 1993. Stable carbon and oxygen isotopes in soil carbonates. In: Swart, P., McKenzie, J.A., Lohman, K.C. (eds.): American Geophysical Union Monograph 78, 217-231.

Cerling, T.E., Harris, J.M., 1999. Carbon isotope fractionation between diet and bioapatite in ungulate mammals and implications for ecological and paleoecological. Oecologia 120, 347–363.

Cerling, T. E., Wang, Y., Quade, J., 1993. Expansion of $C_4$ ecosystems as an indicator of global ecological change in the late Miocene. Nature 361, 344–345.

Cerling, T.E., Harris, J.M., MacFadden, B.J., Leakey, M.G., Quade, J., Eisenmann, V., Ehleringer, J.R., 1997. Global vegetation change through the Miocene/Pliocene boundary. Nature 389, 153–158.

Chen, G., 2002. Late neogene macromammalian assemblage from Lingtai, Gansu Province, China. Vertebrata PalAsiatica 40, 70–79.

DeNiro, M.J., Epstein, S., 1978. Influence of diet on the distribution of carbon isotopes in animals. Geochimica et Cosmochimica Acta 42, 495-506.

Ding, Z.L., Yang, S.L., 2000. $C_3/C_4$ vegetation evolution over the last 7.0 Myr in the Chinese Loess Plateau: Evidence from pedogenic carbonate $\delta^{13}C$. Palaeogeography, Palaeoclimatology, Palaeoecology 160, 291–299.

Ding, Z.L., Xiong, S.F., Sun, J.M., Yang, S.L., Gu, Z.Y., Liu, T.S., 1999. Pedostratigraphy and paleomagnetism of a ~7.0 Ma eolian loess–red clay sequence at Lingtai, Loess Plateau, northcentral China and the implications for paleomonsoon evolution. Palaeogeography, Palaeoclimatology, Palaeoecology 152, 49–66.

Dong, W., Qi, G.-Q., 2013. Hominoid-producing localities and biostratigraphy in China. In Wang, X.-M., Flynn, L.J, Fortelius, M. (Eds.), Fossil Mammals of Asia – Neogene Biostratigraphy and Chronology. Columbia University Press, New York, p. 293–313.

Ehleringer, J.R., Björkman, O., 1977. Quantum yields for $CO_2$ uptake in $C_3$ and $C_4$ plants. Plant Physiology 59, 86-90.

Ehleringer, J.R., Cerling, T.E., Helliker, B.R., 1997. $C_4$ photosynthesis, atmospheric $CO_2$, and climate. Oecologia 112, 285-299.

Eisenberg J., 1981. The mammalian radiations: analysis of trends in evolution,adaptation, and behaviour. The University of Chicago Press, Chicago.

Eronen, J.T., Puolamäki, K., Liu, L., Lintulaakso, K., Damuth, J., Janis, C., Fortelius, M., 2010. Precipitation and large herbivorous mammals , part II: Application to fossil data. Evolutionary Ecology Research 12, 235-248.

Eronen, J.T., Fortelius, M., Micheels, A., Portmann, F.T., Puolamäki, K., Janis, C.M., 2012. Neogene aridification of the Northern Hemisphere. Geology 40, 823–826.

Eronen, J.T., Kaakinen, A., Liu, L., Passsey, B.H., Tang, H., Zhang, Z.Q., 2014. Here be dragons: Mesowear and tooth enamel isotopes of the classic Chinese “Hipparion” Faunas from Baode, Shanxi Province, China. Annales Zoologici Fennici 51, 227–244.

Fabre, P.-H., Hautier, L., Dimitrov, D., Douzery, E.J.P., 2012. A glimpse on the pattern of rodent diversification: a phylogenetic approach. BMC Evolutionary Biology 12, 88.

Flynn, L., Qi, G., 1982. Age of Lufeng, China, hominoid locality. Nature 298, 746–747.

Flynn, L., Wu, W., Downs, W., 1997. Dating microfaunas in the late Neogene record of Northern China. Palaeogeography, Palaeoclimatology, Palaeoecology 133, 227-242

Fortelius, M. (coordinator) 2014. New and Old Worlds Database of Fossil Mammals (NOW). University of Helsinki. http://www.helsinki.fi/science/now/.

Fortelius, M., Zhang, Z., 2006. An Oasis in the desert? : History of endemism and climate in the late Neogene of North China Palaeontographica. Abt. A: Palaeozoologie – Stratigraphie 277, 131-141.

Fortelius, M., Eronen, J.T., Liu, L., Pushkina, D., Rinne, J., Tesakov, A., Vislobokova, I., Zhang, Z., Zhou, L., 2002. Fossil mammals resolve regional patterns of Eurasian climate change during 20 million years. Evolution Ecology Research 4, 1005–1016.

Fortelius, M., Eronen, J.T., Kaya, F., Tang, H., Raia, P., Puolamäki, K., 2014. Evolution of Neogene mammals in Eurasia: environmental forcing and biotic interactions. Annual Reviews of Earth and Planetary Science 42, 579-604.

Fox, D. L., P. L. Koch. 2004. Carbon and oxygen isotope variability in Neogene paleosol carbonates: constraints on the evolution of the $C_4$-grasslands of the Great Plains, USA. Palaeogeography, Palaeoclimatology, Palaeoecology 207, 305–329.

Fox, D.L., Koch, P.L., 2003. Tertiary history of C4 biomass in the Great Plains, USA. Geology 31, 809-812.

Fox, D.L., Honey, J.G., Martin, R.A., Peláez-Campomanes, P., 2012. Pedogenic carbonate stable isotope record of environmental change during the Neogene in the southern Great Plains, southwest Kansas, USA: Carbon isotopes and the evolution of $C_4$-dominated grasslands. Geological Society of America Bulletin 124 444-462.

Fung, I., Field, C.B., Berry, J.A., Thompson, Randerson, J.T., Malmström, C.M., Vitousek, P.M., Collatz, G.J., Sellers, P.J., Randall, D:A., Denning, A.S., Badeck, F., John, J., 1997. Carbon-13 exchanges between the atmosphere and biosphere. Global Biogeochemical Cycles 11, 507– 533.

Gaboardi, M., Deng, T., Wang, Y., 2005. Middle Pleistocene climate and habitat change at Zhoukoudian, China, from the carbon and oxygen isotopic record from herbivore tooth enamel. Quaternary Research 63, 329–338.

Gehler, A., Tütken, T., Pack, A., 2012. Oxygen and carbon isotope variations in a modern rodent community – Implications for palaeoenvironmental reconstructions. PLoSONE 7, e49531.

Grimes S.T., Hooker, J.J., Collinson, M.E., Mattey, D.P., 2005. Summer temperatures of late Eocene to early Oligocene freshwaters. Geology 33, 189–192.

Harrison, T., Ji, X., Su, D., 2002. On the systematic status of the late Neogene hominoids from Yunnan Province, China. Journal of Human Evolution 43, 207–227.

Hopley, P.J., Latham, A.G., Marshall, J.D., 2006. Palaeoenvironments and palaeodiets of mid-Pliocene micromammals from Makapansgat Limeworks, South Africa: A stable isotope and dental microwear approach. Palaeogeography, Palaeoclimatology, Palaeoecology 233, 235–251.

Hynek, S.A., Passey, B.H., Prado, J.L., Brown, F.H., Cerling, T.E., Quade, J., 2012. Small mammal carbon isotope ecology across the Miocene – Pliocene boundary, northwest Argentina. Earth and Planetary Science Letters 321–322, 177–188.

Janis, C.M., Damuth, J., Theodor, J.M., 2000. Miocene ungulates and terrestrial primary productivity: Where have all the browsers gone? Proceedings of the National Academy of Sciences U.S.A. 97, 7899–7904.

Janis, C.M., Damuth, J., Theodor, J.M., 2004. The species richness of Miocene browsers, and implications for habitat type and primary productivity in the North American grassland biome. Palaeogeography, Palaeoclimatology, Palaeoecology 207, 371–398.

Jia, G. D., Pleng, P. A., Zhao, Q. H., Jiang, Z. M., 2003. Changes in terrestrial ecosystem since 30 Ma in East Asia: stable isotope evidence from black carbon in the South China Sea. Geology 31, 1093–1096.

Jiang,W.Y., Peng, S.Z., Hao, Q.Z., Liu, D.S., 2002. Carbon isotopic records in paleosols over the Pliocene in Northern China: implication on vegetation development and Tibetan uplift. Chinese Science Bulletin 47, 687–690.

Jim, S., Ambrose, S.H., Evershed, R.P., 2004. Stable carbon isotopic evidence for differences in the dietary origin of bone cholesterol, collagen, and apatite: implications for their use in palaeodietary reconstruction, Geochimica Cosmochimica Acta 68, 61-72.

Kaakinen, A., Sonninen, E., Lunkka, J.P., 2006. Stable isotope record in paleosol carbonates from the Chinese Loess Plateau: implications for late Neogene paleoclimate and paleovegetation. Palaeogeography, Palaeoclimatology, Palaeoecology 237, 359–369.

Kaakinen, A., Passey, B.H., Zhang Z., Liu, L., Pesonen, L.J., Fortelius, M., 2013: Stratigraphy and paleoecology of the classical dragon bone localities of Baode County, Shanxi Province. In Wang, X., Flynn, L.J., Fortelius, M. (Eds.), Fossil Mammals of Asia – Neogene Biostratigraphy and Chronology. Columbia University Press, New York, p. 203–217.

Keeley, J.E., Rundel, P.W. 2005. Fire and the Miocene expansion of C4 grasslands. Ecology Letters 8, 683-690.

Kimura, Y., Jacobs, L.L., Cerling, T.E., Uno, K.T., Ferguson, K.M., Flynn, L.J., Patnaik, R., 2013. Fossil mice and rats show isotopic evidence of niche partitioning and change in dental ecomorphology related to dietary shift in late Miocene of Pakistan. PlosOne 8(8): e69308

Kita, Z., Secord, R., Boardman, G.S., 2014. A new stable isotope record of Neogene paleoenvironments and mammalian paleoecologies in the western Great Plains during the expansion of $C_4$ grasslands. Palaeogeography, Palaeoclimatology, Palaeoecology 399, 160-172.

Latorre, C., Quade, J., McIntosh, W. C., 1997. The expansion of $C_4$ grasses and global change in the late Miocene: Stable isotope evidence from the Americas. Earth and Planetary Science Letters 146, 83–96.

Leite, R.N., Kolokotronis, S.-O., Almeida, F.C., Werneck, F.P., Rogers, D.S., Weksler, M., 2014. In the wake of invasion: tracing the historical biogeography of the South American cricetid radiation (Rodentia, Sogmodontinae). PLoS ONE 9, e100687.

Lloyd, J., Farquhar, G.D., 1994. $^{13}C$ discrimination during $CO_2$ assimilation by the terrestrial biosphere, Oecologia, 99, 201–215.

Lunt, D.J., Ross, I., Hopley, P.J., Valdes, P.J., 2007. Modelling late Oligocene $C_4$ grasses and climate: Palaeogeography, Palaeoclimatology, Palaeoecology 251, 239–253.

Ma Y.Z., Wu F.L., Fang X.M., Li J.J., An Z.S., Wang W., 2005. Pollen record from red clay sequence in the central Loess Plateau between 8.10 and 2.60 Ma. Chinese Science Bulletin 50, 2234-2243.

MacFadden, B.J., Wang, Y., Cerling, T.E., Anaya, F., 1994. South american fossil mammals and carbon isotopes: a 25 million-year sequence from the Bolivian Andes. Palaoegeography Palaeoclimatology Palaeoecology 107, 257–268.

MacFadden, B.J., Cerling, T.E., Prado, J., 1996. Cenozoic terrestrial ecosystem evolution in Argentina: evidence from carbon isotopes of fossil mammal teeth. Palaios 11, 319–327.

Martin, R. A., Peláez-Campomanes, P. , Honey, J. G. , Fox, D. L. , Zakrzewski, R. J., Albright, L. B. , Lindsay, E. H. Opdyke, N. D. , Goodwin, H. T., 2008. Rodent community change at the Pliocene–Pleistocene transition in southwestern Kansas and identification of the Microtus immigration event on the Central Great Plains. Palaeogeography, Palaeoclimatology, Palaeoecology 267, 196–207.

McInerney, F.A., Strömberg, C.A.E., White, J.W.C., 2011. The Neogene transition from $C_3$ to $C_4$ grasslands in North America: stable carbon isotope ratios of fossil phytoliths. Paleobiology 37, 23-49.

Mirzaie Ataabadi, M., Liu, L., Eronen, J. T., Bernor, R., Fortelius, M., 2013. Continental Scale Patterns in Neogene Mammal Community Evolution and Biogeography: A Europe-Asia Perspective. In Wang, X., Flynn, L.J., Fortelius, M. (Eds), Fossil Mammals of Asia: Neogene Biostratigraphy and Chronology. Columbia University Press, New York, p. 629-655.

Molnar, P., Boos, W. R., Battisti, D. S., 2010. Orographic controls on climate and paleoclimate of Asia: Thermal and mechanical roles for the Tibetan Plateau, Annual Reviews of Earth and Planetary Science 38, 77-102.

Ni, X., Qiu, Z., 2002. The micromammalian fauna from the Leilao, Yuanmou hominoid locality: Implications for biochronology and paleoecology. Journal of Human Evolution 42, 535–546.

Opdyke, N. D., Huang, K., Tedford, R. H., 2013. Erratum to: The paleomagnetism and magnetic stratigraphy of the Late Cenozoic sediments of the Yushe basin, Shanxi Province, China. In Tedford, R. H., Qiu, Z. X., Flynn, L, J. (Eds), Late Cenozoic Yushe Basin, Shanxi Province, China: Geology and Fossil Mammals. Volume 1: History, Geology, and Magnetostratigraphy. Springer.

Pagani, M.P., Arthur, M.A., Freeman, K.H. 1999. Miocene evolution of atmospheric carbon dioxide. Paleoceanography 14, 273–292.

Passey, B.H., 2007. Stable isotope paleoecology: methodological advances and applications to the Late Neogene environmental history of China. Dissertation. Department of Geology and Geophysics, The University of Utah, pp. 266.

Passey, B.H. and Cerling, T.E., 2006. In situ stable isotope analysis ($\delta^{13}C$, $\delta^{18}O$) of very small teeth using laser ablation GC/IRMS. Chemical Geology 235, 238–249.

Passey, B.H., Cerling, T.E., Perkins, M.E., Voorhies, M.R., Harris, J.M., Tucker S.T., 2002. Environmental change in the Great Plains: an isotopic record from fossil horses. Journal of Geology 110, 123–140

Passey, B.H., Robinson, T.F., Ayliffe, L.K., Cerling, T.E., Sponheimer, M., Dearing, M.D., Roeder, B.L., Ehleringer J.R., 2005. Carbon isotope fractionation between diet, breath $CO_2$, and bioapatite in different mammals. Journal of Archaeological Science 32, 1459–1470.

Passey, B.H., Ayliffe, L.K., Kaakinen, A., Zhang, Z., Eronen, J.T., Zhu, Y., Zhu, L., Cerling, T.E., Fortelius, M. 2009. Strengthened East Asian summer monsoons during a period of high-latitude warmth? Isotopic evidence from Mio-Pliocene fossil mammals and soil carbonates from northern China. Earth and Planetary Science Letters 277, 443–452.

Podlesak, D.W., Torregrossa, A.-M., Ehleringer, J.R., Dearing, M.D., Passey, B.H., Cerling T.E., 2008. Turnover of oxygen and hydrogen isotopes in the body water, $CO_2$, hair, and enamel of a small mammal. Geochimica et Cosmochimica Acta 72, 19–35.

Qi, G., Dong, W., Zheng, L., Zhao, L., Gao, F., Yue, L., Zhang Y., 2006. Taxonomy, age and environment status of the Yuanmou hominoids. Chinese Science Bulletin 51, 704–712.

Qiu, Z. D., Wang, X. M., Li, Q., 2006. Faunal succession and biochronology of the Miocene through Pliocene in Nei Mongol (Inner Mongolia). Vertebrata PalAsiatica 44, 164-181

Qiu, Z.-D., Wang, X.-M. Li, Q., 2013. Neogene faunal succession and biochronology of Central Nei Mongol (Inner Mongolia). In Wang, X.-M., Flynn, L.J, Fortelius, M. (Eds.), Fossil Mammals of Asia – Neogene Biostratigraphy and Chronology. Columbia University Press, New York, 155–186.

Qiu, Z.-X., Qiu, Z.-D., Deng, T., Li, C.-K., Zhang, Z.-Q., Wang, B.-Y., Wang, X.-M., 2013. Neogene land mammals stages/ages of China –toward the goal to establish an Asian Land mammal stage/age schemeIn Wang, X.-M., Flynn, L.J and Fortelius, M. (eds.), Fossil Mammals of Asia – Neogene Biostratigraphy and Chronology. Columbia University Press, New York, p. 29–90.

Quade, J., Cerling, T.E., 1995. Expansion of $C_4$ grasses in the late Miocene of northern Pakistan: evidence fromstable isotopes in paleosols. Palaoegeography, Palaeoclimatology, Palaeoecology 115, 91–116.

Quade J, Cerling T.E, Bowman J.R., 1989. Development of the Asian Monsoon revealed by marked ecological shift in the latest Miocene in northern Pakistan. Nature 342, 163–166

Quade, J., Cerling, T.E., Barry, J.C., Morgan, M.E., Pilbeam, D.E., Chivas, A.R., Lee-Thorp, J.A., van der Merwe, N.J., 1992. A 16-Ma record of paleodiet using carbon and oxygen isotopes in fossil teeth from Pakistan. Chemical Geology 94, 183-192.

Quade, J., Cater, J.M.L., Ojha, T.P., Adam, J., Harrison, T.M., 1995. Late Miocene environmental change in Nepal and the northern Indian subcontinent: stable isotopic evidence from paleosols. Geological Society of America Bulletin 107, 1381–1397.

Ramage, C., 1971. Monsoon Meteorology, International Geophysics Series, 15. Academic Press, San Diego.

Rao, W., Chen, J., Yang, J., Ji, J., Zhang, G., Chen, J., 2008. Strontium isotopic and elemental characteristics of calcites in the eolian dust profile of the Chinese Loess Plateau during the past 7 Ma. Geochemical Journal 42, 493-506.

Rea, D.K., Snoeckx, H., Joseph, L.H., 1998. Late Cenozoic eolian deposition in the North Pacific: Asian drying, Tibetan uplift, and cooling of the northern hemisphere. Paleoceanography 13, 215–224.

Sanyal, P., Bhattacharya, S.K., Kumar, R., Ghosh, S.K., Sangode, S.J., 2004. Mio–Pliocene monsoonal record from Himalayan foreland basin (Indian Siwalik) and its relation to the vegetational change. Palaeogeography, Palaeoclimatology, Palaeoecology 205, 23–41.

Scheiter, S., Higgins, S.I., Osborne, C.P., Bradshaw, C., Lunt, D., Ripley, B.S., Taylor, L.L., Beerling, D.J., 2012. Fire and fire-adapted vegetation promoted C4 expansion in the late Miocene. New Phytologist 195, 653-666.

Schenk, J.J., Rowe, K.C., Steppan, S.J., 2013. Ecological opportunity and incumbency in the diversification of repeated continental colonizations by muroid rodents. Systematic Biology 62, 837-864.

Schlosser, M., 1924. Tertiary vertebrates from Mongolia. Paleontologia Sinica, series C1(1), 1–119.

Ségalen L., Lee-Thorp, J.A., Cerling, T., 2007. Timing of $C_4$ grass expansion across sub-Saharan Africa. Journal of Human Evolution 53, 549–559.

Sharp, Z.D. and Cerling, T.E., 1996. A laser GC-IRMS technique for in situ stable isotope analyses of carbonates and phosphates. Geochimica et Cosmochimica Acta 60, 2909-2916.

Singh, S., Parkash, B., Awasthi, A.K., Kumar, S., 2011. Late Miocene record of palaeovegetation from Siwalik palaeosols of the Ramnagar sub-basin, India. Current Science 100, 213–222.

Singh, S., Awasthi, A.K., Parkash, B., Kumar, S., 2013. Tectonics or climate: What drove the Miocene global expansion of $C_4$ grasslands? International Journal of Earth Sciences (Geologische Rundschau) 102, 2019–2031.

Still, C.J., Berry, J.A., Collatz, G.J., DeFries, R.S., 2003. Global distribution of $C_3$ and $C_4$ vegetation: Carbon cycle implications. Global Biogeochemical Cycles 17, 1006, doi:10.1029/2001GB001807.

Storch, G., 1987. The Neogene mammalian faunas of Ertemte and Harr Obo in Inner Mongolia (Nei Mongol), China. 7. Muridae (Rodentia). Senckenbergiana lethaea 67, 401-431

Strömberg, C.A.E., 2005. Decoupled taxonomic radiation and ecological expansion of open-habitat grasses in the Cenozoic of North America. Proceedings of the National Academy of Sciences U.S.A. 102, 11980-11984.

Strömberg, C.A.E., 2011. Evolution of grasses and grassland ecosystems. Annual Review of Earth and Planetary Sciences 39, 517–544.

Strömberg, C.A.E., McInerney, F.A., 2011. The Neogene transition from $C_3$ to $C_4$ grasslands in North America: assemblage analysis of fossil phytoliths. Paleobiology 37, 50–71.

Suarez, M.B., Passey, B.H., Kaakinen, A., 2011. Paleosol carbonate multiple isotopologue signature of active East Asian summer monsoons during the late Miocene and Pliocene. Geology 39, 1151-1154.

Sun, X., Wang, P., 2005, How old is the Asian monsoon system?—Palaeobotanical records from China. Palaeogeography, Palaeoclimatology, Palaeoecology 222, 181-222.

Sun, Y., An, Z., Clemens, S. C., Bloemendal, J., Vandenberghe, J., 2010: Seven million years of wind and precipitation variability on the Chinese Loess Plateau. Earth and Planetary Science Letters 297, 525–535.

Tang, H., 2013. The spatio-temporal evolution of the Asian monsoon climate in the Late Miocene and its causes: A regional climate model study. PhD Thesis, Unigrafia, Helsinki, 50 pp.

Tang, H., Eronen, J.T., Kaakinen, A., Utescher, T., Ahrens, B., Fortelius, M., 2015. Strong winter monsoon wind causes surface cooling over India and China in the Late Miocene. Climate of the Past Discussions 11, 63–93.

Tieszen, L. L., Fagre, T., 1993. Effect of diet quality and composition on the isotopic composition of respiratory CO2, bone collagen, bioapatite, and soft tissues. In J. B. Lambert and G. Grupe (Eds), Prehistoric Human Bone Archaeology at the Molecular Level). Springer-Verlag, pp. 120–155.

Tipple, B.J., Pagani, M., 2007. The Early Origins of Terrestrial C4 Photosynthesis. Annual Review Earth and Planetary Sciences 35, 435–461

Uno, K.T., Cerling, T.E., Harris, J.M., Kunimatsu, Y., Leakey, M.G., Nakatsukasa, M., Nakaya, H., 2011. Late Mioce to Pliocen carbon isotope record of differential diet change among East African herbivores. Proceedings of the National Academy of Science of the U. S. A. 108, 6509–6514.

Urban, M.A., Nelson, D.M., Jiménez-Moreno, G., Châteauneuf, J.-J., Pearson, A., Hu, F.S., 2010. Isotopic evidence of $C_4$ grasses in southwestern Europe during the Early Oligocene -Middle Miocene. Geology 38, 1091-1094.

Vicentini, A., Barber, J.C., Aliscioni, S.S., Giussani, L.M., Kellogg, E.A., 2008. The age of the grasses and clusters of origins of $C_4$ photosynthesis. Global Change Biology 14, 2963–2977.

Wang L., Lu H. Y., Wu N. Q., Li J., Pei Y. P., Tong G. B., Peng S. Z., 2006. Palynological evidence for Late Miocene-Pliocene vegetation evolution recorded in the red clay sequence of the central Chinese Loess Plateau and implication for palaeoenvironmental change. Palaeogeography, Palaeoclimatology, Palaeoecology 241, 118-128.

Wang, P.X., Clemens, S., Beaufort, L., Braconnot, P., Ganssen, G., Jian, Z. M., Kershaw, P., Sarnthein, M., 2005. Evolution and variability of the Asian monsoon system: state of the art and outstanding issues, Quaternary Science Reviews 24, 595–629.

Wang, Y., Deng, T., 2005. A 25 m.y. isotopic record of paleodiet and environmental change from fossil mammals and paleosols from the NE margin of the Tibetan Plateau. Earth and Planetary Science Letters 236, 322–338.

Wang, Y., Cerling, T. E., MacFadden, B. J., 1994. Fossil horses and carbon isotopes: new evidence for Cenozoic dietary, habitat, and ecosystem changes in North America. Palaeogeography, Palaeoclimatology, Palaeoecology 107, 269–279.

Webster,P.J., Magaña, V.O., Palmer, T.N., Shukla, J., Tomas, R.A., Yanai, M., Yasunari, T., 1998. Monsoons: processes, predictability, and the prospects for prediction. Journal of Geophysical Research 103, 14451-14510.

Wei, L.Y., Chen, M.Y., Zhao, H.M., Sun, J.M., Lu, X., 1993. Magnetostratigraphic study on the late Miocene–Pliocene lacustrine sediments near Leijiahe. In: Monograph of the meeting in honor of Prof. Yuan Fuli on the hundredth anniversary of his birth, p. 63–67, Seismological Press, Beijing. (in Chinese).

WorldClim Dataset, http://worldclim.org

Wu, N.Q., Pei, Y.P., Lu, H.Y., Guo, Z.T., Li, F. J., Liu, T.S., 2006. Marked ecological shifts during 6.2-2.4 Ma revealed by a terrestrial molluscan record from the Chinese Red Clay Formation and implication for palaeoclimatic evolution. Palaeogeography, Palaeoclimatology, Palaeoecology 233, 287-299.

Xing, Y., Utescher, T., Jacques, F.M.B., Su, T., Liu, Y.C., Huang, Y., Zhou, Z., 2012. Palaeoclimatic estimation reveals a weak winter monsoon in southwestern China during late Miocene: evidence from plant macrofossils. Palaeogeography, Palaeoclimatology, Palaeoecology 358-360, 19-25.

Yeakel, J.D., Bennett, N.C., Koch, P.L., Dominy, N.J., 2007. The isotopic ecology of African mole rats informs hypotheses on the evolution of human diet. Proceedings of the Royal Society (B) 274, 1723–1730.

Yin, J., 1994. The Late Cenozoic paleomagnetic chronostratigraphy of Yuanmou Basin and its paleontological significance. Yunnan Geology 13, 306–311.

Yue, L., Zhang, Y., Qi, G., Heller, F.A., Wang, J., Yang, L., Zhang, R., 2004. Paleomagnetic age and palaeobiological significance of hominoid fossil strata of yuanmou Basin in Yunnan. Science in China Series D Earth Sciences 47, 405–411.

Zazzo, A., Balasse, M., Passey, B.H., Moloney, A.P., Monahan, F.J., Schmidt, O., 2010. The isotope record of short- and long-term dietary changes in sheep tooth enamel: implications for quantitative reconstruction of paleodiets. Geochimica et Cosmochimica Acta 74, 3571–3586.

Zhang, C., Wang, Y., Deng, T., Wang X., Biasatti, D., Xu, Y., Li, Q., 2009. $C_4$ expansion in the central Inner Mongolia during the latest Miocene and early Pliocene. Earth and Planetary Science Letters 287, 311–319.

Zhang Z., Kaakinen, A., Liu L., Lunkka, J.P., Sen, S., Qiu Z., Zheng, S., Fortelius, M., 2013. Mammalian biochronology of the Late Miocene Bahe Formation. In Wang, X., Flynn, L.J and Fortelius, M. (Eds.), Fossil Mammals of Asia – Neogene Biostratigraphy and Chronology. Columbia University Press, New York, 203–217.

Zheng, S., Zhang, Z., 2001. Late Miocene–Early Pleistocene biostratigraphy of the Leijiahe area, Lingtai, Gansu. Vertebrata PalAsiatica 39, 215–228.

**FIGURES**

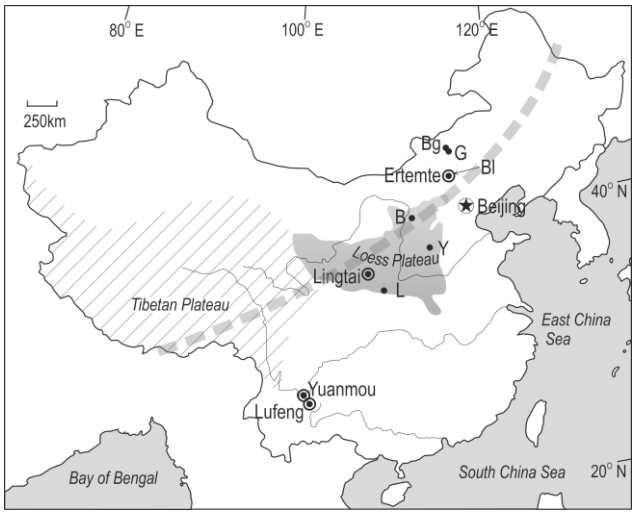


Figure 1. Map showing the sampled Neogene fossil localities. Additionally, the locations of five other sites discussed in the text are indicated; L=Lantian, Y=Yushe, B=Baode, Bl=Bilike, G=Gaotege, Bg=Baogedawula. Dashed line indicates the approximate northwesterly extent of the present-day summer monsoon.

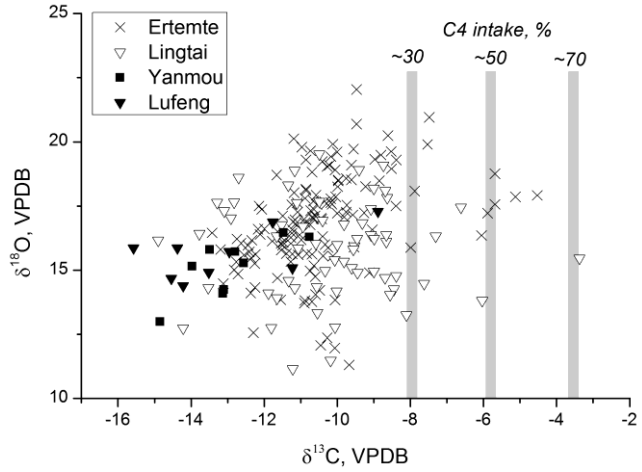


Figure 2. $\delta^{13}C$ and $\delta^{18}O$ values of rodent tooth enamel. Each symbol represents the mean value of one to four analyses of an individual tooth. Error bars are excluded for clarity, but are generally less than 1‰ (1σ) for both $\delta^{13}C$ and $\delta^{18}O$. $\delta^{13}C$ values are adjusted by +0.5 ‰ to account for the mean offset between laser-based and conventional phosphoric acid digestion-based $\delta^{13}C$ values (see Material & Methods). Proportions of consumed C4 vegetation were calculated following the approach of Passey et al. (2002), using an enamel-diet fractionation of 11.0‰.

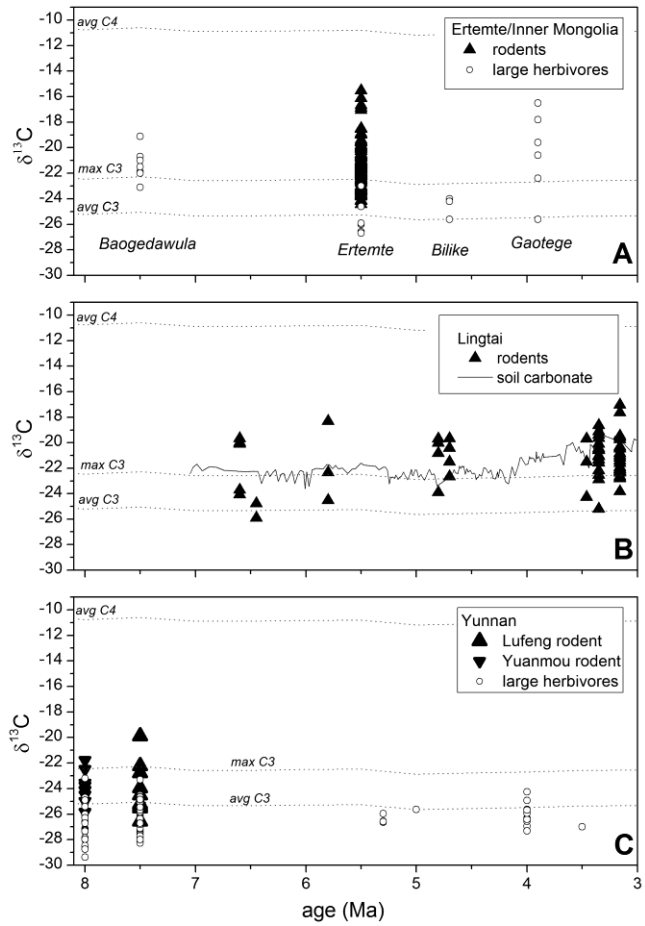


Figure 3. Records of $\delta^{13}C$ of vegetation in the diets of fossil mammals from China – Ertemte and Inner Mongolia (A), Lingtai (B) and Yunnan (C). Large mammal data for Inner Mongolia from Zhang et al., (2009) and for Yunnan from Passey (2007) and Biasatti et al. (2012). Soil carbonate data for Lingtai from Ding and Yang (2000). The dotted lines indicate model-predicted (Passey et al., 2009) $\delta^{13}C$ values of average C3 vegetation, water-stressed plants and average C4 plants. The late Miocene large mammal data from Biasatti et al. (2012) and Passey (2007) are plotted according to the age estimates given in the text (section 2 Regional Setting) instead of those used in the original publications.

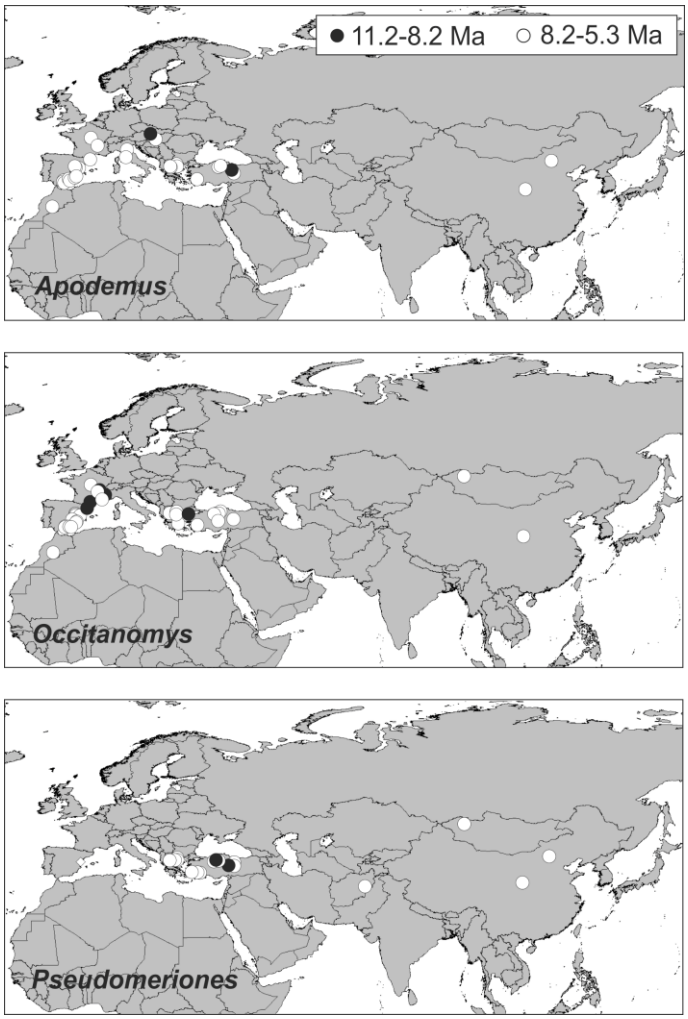


Figure 4. Recorded occurrences of the ”high-$C_4$” genera *Apodemus*, *Occitanomys* and *Pseudomeriones* for 11.2-8.2 Ma (black dots) and 8.2-5.3 Ma (white dots) in the NOW database (Fortelius, 2014).

Table 1. Sample material, number of tooth specimens analyzed per taxon, range of enamel $\delta^{13}C$ values and calculated contribution of C4 grasses to diet.

| | | n | $\delta^{13}C$ range[a] max | min | %C4[b] |
|---|---|---|---|---|---|
| **ERTEMTE, INNER MONGOLIA** | | | | | |
| **Cricetidae** | *Sinocricetus zdanskyi* | 10 | -9.5 | -10.9 | 7-18 |
| | *Sinocricetus* sp. | 10 | -5.9 | -11.5 | 1-49 |
| | *Microtodon atavus* | 8 | -10.6 | -12.6 | 0-9 |
| | *Pseudomeriones abbreviatus* | 7 | -4.5 | -11.1 | 5-60 |
| | *Kowalskia neimengensis* | 5 | -10.3 | -11.8 | 0-11 |
| | *Microtoscoptes praetermissus* | 5 | -11.2 | -13.1 | 0-4 |
| | *Nannocricetus* sp. | 5 | -8.5 | -11.0 | 5-26 |
| | *Anatolomys teilhardi* | 2 | -11.2 | -11.3 | 3 |
| **Cricetidae (Myospalacinae)** | *Prosiphneus licenti* | 5 | -10.9 | -12.2 | 0-6 |
| **Dipodidae** | *Dipus fraudator* | 9 | -7.5 | -10.7 | 8-35 |
| | *Lophocricetus* sp. | 8 | -8.4 | -11.0 | 1-27 |
| | *Paralactaga suni* | 4 | -9.0 | -11.3 | 3-18 |
| | *Prolophocricetus* sp. | 3 | -9.3 | -12.6 | 0-20 |
| | *Sicista* sp. | 1 | -11.2 | | 4 |
| | *Sinozapus* sp. | 1 | -11.3 | | 3 |
| **Muridae** | *Occitanomys pusillus* | 15 | -5.7 | -12.4 | 0-50 |
| | *Apodemus orientalis* | 7 | -5.1 | -12.3 | 0-55 |
| | *Micromys chalceus* | 5 | -11.5 | -13.4 | 0-1 |
| | *Karnimata hipparionum* | 4 | -10.2 | -13.2 | 0-12 |
| | *Orientalomys* cf. *similis* | 3 | -10.9 | -12.1 | 0-7 |
| **Ochotonidae** | *Ochotona lagreli* | 8 | -9.1 | -10.1 | 13-21 |
| | *Ochotona minor* | 5 | -10.1 | -10.7 | 8-13 |
| **Sciuridae** | *Eutamias ertemtensis* | 8 | -10.0 | -12.1 | 0-14 |
| | *Sinotamias* sp. | 1 | -12.8 | | 0 |
| | *Prospermophilus* sp. | 1 | -10.4 | | 11 |
| **Gliridae** | *Myomimus sinensis* | 2 | -11.1 | -11.7 | 0-5 |
| **LINGTAI, GANSU PROVINCE** | | | | | |
| **Cricetidae** | *Pseudomeriones abbreviatus* | 15 | -3.4 | -14.9 | 0-73 |
| | *Bahomys* sp. | 7 | -8.7 | -13.3 | 0-25 |
| | *Nannocricetus* sp. | 4 | -6.0 | -10.2 | 13-48 |
| | *Allocricetus bursae* | 4 | -8.6 | -11.1 | 5-27 |
| | *Chardinomys primitivus* | 3 | -8.7 | -12.7 | 0-26 |
| **Cricetidae (Myospalacinae)** | *Mesosiphneus intermedius* | 4 | -11.1 | -11.8 | 0-5 |
| | *Mesosiphneus teilhardi* | 3 | -10.5 | -11.2 | 5-10 |
| | *Prosiphneus licenti* | 3 | -8.4 | -9.1 | 19-28 |
| **Ochotonidae** | *Ochotona* sp. | 14 | -7.6 | -11.9 | 0-35 |
| | *Ochotonoides complicidens* | 4 | -8.1 | -14.2 | 0-30 |
| **Muridae** | *Karnimata hipparionum* | 3 | -9.0 | -13.1 | 0-23 |
| **YUANMOU, YUNNAN PROVINCE** | | | | | |
| **Platacanthomyidae** | *Platacanthomys dianensis* | 2 | -11.5 | -12.6 | 0-1 |

| | | | | | |
|---|---|---|---|---|---|
| | *Typhlomys primitivus* | 3 | -12.8 | -13.5 | 0 |
| **Muridae** | *Linomys yunnanensis* | 4 | -10.8 | -14.8 | 0-7 |
| **LUFENG, YUNNAN PROVINCE** | | | | | |
| **Muridae** | *Linomys yunnanensis* | 6 | -8.9 | -15.6 | 0-23 |
| **Cricetidae** | *Kowalskia hanae* | 3 | -13.5 | -14.5 | 0 |

The full data, including ages of sampled material, are given in the Appendix.

[a] Values have been adjusted by +0.5‰ to account for the mean offset between laser-based and conventional phosphoric acid digestion-based $\delta^{13}C$ values (see Material and Methods).

[b] Proportions of C4 vegetation are calculated following Passey et al. (2002) (see Material and Methods).

**Appendix. Carbon isotope values of Late Miocene to Pliocene mammals from China.**

**A) Small mammal carbon isotope values (this study)**

| Locality | Age (Ma) | Taxon | Sample ID | n [a] | $\delta^{13}C_{laser}$ | stdev $\delta^{13}C$ | $\delta^{13}C_{adj.}$ [b] | C4% | $\delta^{18}O$ | stdev $\delta^{18}O$ |
|---|---|---|---|---|---|---|---|---|---|---|
| **Ertemte** | | | | | | | | | | |
| | 5.5 | Ochotona lagreli | ER_Pro1 | 2 | -10.2 | 0.0 | -9.7 | 17 | 11.3 | 0.1 |
| | 5.5 | Ochotona lagreli | ER_Pro2 | 3 | -9.6 | 0.1 | -9.1 | 21 | 14.9 | 0.3 |
| | 5.5 | Ochotona lagreli | ER_Pro3 | 2 | -10.6 | 0.0 | -10.1 | 13 | 13.8 | 0.0 |
| | 5.5 | Ochotona lagreli | ER_Pro4 | 2 | -9.7 | 0.2 | -9.2 | 20 | 18.3 | 0.0 |
| | 5.5 | Ochotona lagreli | ER_Pro5 | 2 | -10.2 | 0.1 | -9.7 | 16 | 17.5 | 0.3 |
| | 5.5 | Ochotona lagreli | ER_Ola6 | 2 | -10.6 | 0.0 | -10.1 | 13 | 15.6 | 0.0 |
| | 5.5 | Ochotona lagreli | ER_Ola7 | 2 | -10.5 | 0.7 | -10 | 14 | 17.9 | 0.4 |
| | 5.5 | Ochotona lagreli | ER_Ola8 | 2 | -10.1 | 0.2 | -9.6 | 17 | 17.2 | 0.3 |
| | 5.5 | Ochotona minor | ER_Mpr1 | 2 | -10.6 | 0.1 | -10.1 | 13 | 12.0 | 0.1 |
| | 5.5 | Ochotona minor | ER_Mpr2 | 2 | -10.8 | 0.1 | -10.3 | 11 | 12.4 | 0.9 |
| | 5.5 | Ochotona minor | ER_Mpr3 | 1 | -11.1 | | -10.6 | 9 | 14.8 | |
| | 5.5 | Ochotona minor | ER_Mpr4 | 2 | -11 | 0.2 | -10.5 | 10 | 12.1 | 0.3 |
| | 5.5 | Ochotona minor | ER_Mpr5 | 2 | -11.2 | 0.0 | -10.7 | 8 | 13.8 | 1.5 |
| | 5.5 | Prosiphneus licenti | ER_Ola1 | 2 | -12.7 | 0.3 | -12.2 | 0 | 15.6 | 0.3 |
| | 5.5 | Prosiphneus licenti | ER_Ola2 | 2 | -11.4 | 0.0 | -10.9 | 6 | 13.7 | 0.0 |
| | 5.5 | Prosiphneus licenti | ER_Ola3 | 2 | -11.4 | 0.3 | -10.9 | 6 | 13.8 | 0.0 |
| | 5.5 | Prosiphneus licenti | ER_Ola4 | 2 | -12.1 | 0.1 | -11.6 | 0 | 14.7 | 0.1 |
| | 5.5 | Prosiphneus licenti | ER_Ola5 | 2 | -12 | 0.0 | -11.5 | 1 | 13.8 | 0.1 |
| | 5.5 | Paralactaga suni | ER_Psu1 | 4 | -10 | 1.0 | -9.5 | 18 | 20.7 | 0.8 |
| | 5.5 | Paralactaga suni | ER_Psu2 | 2 | -10.1 | 0.2 | -9.6 | 18 | 19.7 | 0.3 |
| | 5.5 | Paralactaga suni | ER-Psu3 | 2 | -10.8 | 0.1 | -10.3 | 11 | 16.0 | 0.0 |
| | 5.5 | Paralactaga suni | ER-Psu4 | 2 | -11.8 | 0.0 | -11.3 | 3 | 16.0 | 0.1 |
| | 5.5 | Dipus fraudator | ER_Sfr1 | 2 | -9.3 | 0.3 | -8.8 | 24 | 19.5 | 0.1 |
| | 5.5 | Dipus fraudator | ER_Sfr2 | 2 | -9.5 | 0.3 | -9 | 22 | 16.6 | 0.1 |
| | 5.5 | Dipus fraudator | ER_Sfr3 | 2 | -10 | 0.6 | -9.5 | 18 | 22.0 | 0.3 |
| | 5.5 | Dipus fraudator | ER_Sfr4 | 2 | -8.9 | 0.1 | -8.4 | 27 | 19.3 | 0.0 |
| | 5.5 | Dipus fraudator | ER_Sfr5 | 2 | -9.1 | 0.9 | -8.6 | 26 | 20.2 | 0.4 |
| | 5.5 | Dipus fraudator | ER_Sfr6 | 3 | -9 | 0.5 | -8.5 | 26 | 19.0 | 0.3 |
| | 5.5 | Dipus fraudator | ER-Sfr7 | 3 | -8 | 0.5 | -7.5 | 35 | 21.0 | 0.3 |
| | 5.5 | Dipus fraudator | ER-Sfr8 | 2 | -8 | 0.3 | -7.5 | 35 | 19.9 | 0.1 |
| | 5.5 | Dipus fraudator | ER-Sfr9 | 2 | -11.2 | 0.5 | -10.7 | 8 | 18.8 | 0.3 |
| | 5.5 | Lophocricetus sp. | ER_Lop1 | 2 | -11.2 | 0.0 | -10.7 | 8 | 17.1 | 0.1 |
| | 5.5 | Lophocricetus sp. | ER_Lop2 | 2 | -10.5 | 0.1 | -10 | 14 | 17.2 | 0.0 |
| | 5.5 | Lophocricetus sp. | ER_Lop3 | 2 | -8.9 | 0.4 | -8.4 | 27 | 17.5 | 0.1 |
| | 5.5 | Lophocricetus sp. | ER_Lop4 | 2 | -10.5 | 0.3 | -10 | 14 | 18.5 | 0.1 |
| | 5.5 | Lophocricetus sp. | ER_Lop5 | 2 | -10.3 | 0.0 | -9.8 | 16 | 18.6 | 0.1 |
| | 5.5 | Lophocricetus sp. | ER_Lop6 | 2 | -11.1 | 0.5 | -10.6 | 9 | 17.9 | 0.6 |
| | 5.5 | Lophocricetus sp. | ER_Lop7 | 2 | -11.4 | 0.0 | -10.9 | 6 | 17.8 | 0.4 |
| | 5.5 | Lophocricetus sp. | ER_Lop8 | 2 | -12 | 0.4 | -11.5 | 1 | 17.1 | 0.1 |
| | 5.5 | Prolophocricetus sp. | ER-Plo1 | 2 | -11.6 | 0.3 | -11.1 | 4 | 16.8 | 0.0 |

| | | | | | | | | | |
|---|---|---|---|---|---|---|---|---|---|
| 5.5 | Prolophocricetus sp. | ER-Plo2 | 2 | -13.1 | 0.1 | -12.6 | 0 | 16.1 | 0.4 |
| 5.5 | Prolophocricetus sp. | ER-Plo3 | 2 | -9.8 | 0.1 | -9.3 | 20 | 17.2 | 0.1 |
| 5.5 | Sicista sp. | ER_Sic1 | 2 | -11.7 | 0.0 | -11.2 | 4 | 18.0 | 0.1 |
| 5.5 | Sinozapus sp. | ER_Szp1 | 3 | -11.8 | 0.3 | -11.3 | 3 | 17.6 | 0.2 |
| 5.5 | Sinocricetus zdanskyi | ER_Szd1 | 2 | -10 | 0.1 | -9.5 | 18 | 15.9 | 0.0 |
| 5.5 | Sinocricetus zdanskyi | ER_Szd2 | 2 | -10.8 | 0.0 | -10.3 | 11 | 17.6 | 0.0 |
| 5.5 | Sinocricetus zdanskyi | ER_Szd3 | 2 | -10.3 | 0.1 | -9.8 | 15 | 17.1 | 0.2 |
| 5.5 | Sinocricetus zdanskyi | ER_Szd4 | 2 | -10.1 | 0.2 | -9.6 | 17 | 18.5 | 0.2 |
| 5.5 | Sinocricetus zdanskyi | ER_Szd5 | 2 | -10.9 | 0.1 | -10.4 | 10 | 19.2 | 0.0 |
| 5.5 | Sinocricetus zdanskyi | ER_Szd6 | 2 | -10.7 | 0.1 | -10.2 | 12 | 19.4 | 0.1 |
| 5.5 | Sinocricetus zdanskyi | ER_Szd7 | 2 | -11.2 | 0.0 | -10.7 | 8 | 16.8 | 0.0 |
| 5.5 | Sinocricetus zdanskyi | ER_Szd8 | 2 | -11.4 | 0.1 | -10.9 | 7 | 18.1 | 0.2 |
| 5.5 | Sinocricetus zdanskyi | ER_Szd9 | 2 | -11.2 | 0.1 | -10.7 | 8 | 15.6 | 0.2 |
| 5.5 | Sinocricetus zdanskyi | ER_Szd10 | 2 | -11.1 | 0.0 | -10.6 | 9 | 14.0 | 0.4 |
| 5.5 | Microtodon atavus | ER_Mat1 | 2 | -12.1 | 0.3 | -11.6 | 0 | 16.5 | 0.2 |
| 5.5 | Microtodon atavus | ER_Mat3 | 2 | -13.1 | 0.1 | -12.6 | 0 | 15.6 | 0.2 |
| 5.5 | Microtodon atavus | ER_Mat5 | 4 | -12.9 | 0.1 | -12.4 | 0 | 14.1 | 0.1 |
| 5.5 | Microtodon atavus | ER_Mat6 | 2 | -11.7 | 0.1 | -11.2 | 4 | 16.9 | 0.1 |
| 5.5 | Microtodon atavus | ER_Mat7 | 2 | -11.6 | 0.0 | -11.1 | 5 | 15.6 | 0.0 |
| 5.5 | Microtodon atavus | ER_Mat8 | 2 | -11.5 | 0.1 | -11 | 5 | 16.2 | 0.0 |
| 5.5 | Microtodon atavus | ER_Mat9 | 2 | -11.1 | 0.0 | -10.6 | 8 | 15.2 | 0.0 |
| 5.5 | Microtodon atavus | ER_Mat10 | 3 | -11.1 | 0.3 | -10.6 | 9 | 17.1 | 0.2 |
| 5.5 | Sinocricetus sp. | ER_Sin1 | 2 | -10.6 | 0.0 | -10.1 | 13 | 17.6 | 0.1 |
| 5.5 | Sinocricetus sp. | ER_Sin2 | 2 | -12 | 0.1 | -11.5 | 1 | 16.1 | 0.0 |
| 5.5 | Sinocricetus sp. | ER_Sin3 | 2 | -11.1 | 0.0 | -10.6 | 9 | 17.6 | 0.0 |
| 5.5 | Sinocricetus sp. | ER_Sin4 | 2 | -10.6 | 0.0 | -10.1 | 13 | 18.9 | 0.0 |
| 5.5 | Sinocricetus sp. | ER_Sin5 | 2 | -10.7 | 0.0 | -10.2 | 12 | 19.1 | 0.1 |
| 5.5 | Sinocricetus sp. | ER_Sin6 | 2 | -11.3 | 0.2 | -10.8 | 7 | 15.6 | 0.1 |
| 5.5 | Sinocricetus sp. | ER_Sin7 | 2 | -11.7 | 0.0 | -11.2 | 3 | 15.6 | 0.1 |
| 5.5 | Sinocricetus sp. | ER_Sin8 | 2 | -9.4 | 0.0 | -8.9 | 24 | 18.5 | 0.1 |
| 5.5 | Sinocricetus sp. | ER_Sin9 | 2 | -10.9 | 0.3 | -10.4 | 10 | 16.3 | 0.1 |
| 5.5 | Sinocricetus sp. | ER_Sin10 | 2 | -6.4 | 0.4 | -5.9 | 49 | 17.2 | 0.4 |
| 5.5 | Microtoscoptes praetermissus | ER_Omi1 | 2 | -12.8 | 0.1 | -12.3 | 0 | 12.6 | 0.1 |
| 5.5 | Microtoscoptes praetermissus | ER_Omi2 | 3 | -11.7 | 0.6 | -11.2 | 4 | 17.0 | 0.3 |
| 5.5 | Microtoscoptes praetermissus | ER_Omi3 | 2 | -12.8 | 0.0 | -12.3 | 0 | 14.3 | 0.1 |
| 5.5 | Microtoscoptes praetermissus | ER_Omi4 | 2 | -13.6 | 0.2 | -13.1 | 0 | 14.5 | 0.1 |
| 5.5 | Microtoscoptes praetermissus | ER_Omi5 | 2 | -13.2 | 0.1 | -12.7 | 0 | 14.9 | 0.0 |
| 5.5 | Kowalskia neimengensis | ER_Kmo1 | 2 | -11.8 | 0.1 | -11.3 | 3 | 16.3 | 0.0 |
| 5.5 | Kowalskia neimengensis | ER_Kmo2 | 2 | -12.3 | 0.2 | -11.8 | 0 | 16.1 | 0.3 |
| 5.5 | Kowalskia neimengensis | ER_Kmo3 | 2 | -10.9 | 0.1 | -10.4 | 10 | 17.0 | 0.0 |
| 5.5 | Kowalskia neimengensis | ER_Kmo4 | 2 | -11.1 | 0.3 | -10.6 | 8 | 17.4 | 0.1 |
| 5.5 | Kowalskia neimengensis | ER_Kmo5 | 2 | -10.8 | 0.2 | -10.3 | 11 | 17.7 | 0.3 |

| | | | | | | | | | |
|---|---|---|---|---|---|---|---|---|---|
| 5.5 | Nannocricetus sp. | ER_Nan1 | 2 | -10.5 | 0.1 | -10 | 14 | 18.5 | 0.2 |
| 5.5 | Nannocricetus sp. | ER_Nan2 | 2 | -11.5 | 0.1 | -11 | 5 | 16.4 | 0.2 |
| 5.5 | Nannocricetus sp. | ER_Nan3 | 2 | -10.8 | 0.3 | -10.3 | 11 | 19.0 | 0.2 |
| 5.5 | Nannocricetus sp. | ER_Nan4 | 3 | -9 | 0.3 | -8.5 | 26 | 19.6 | 0.2 |
| 5.5 | Nannocricetus sp. | ER_Nan5 | 2 | -9.5 | 0.5 | -9 | 23 | 19.3 | 0.1 |
| 5.5 | Anatolomys teilhardi | ER_Ate1 | 2 | -11.7 | 0.1 | -11.2 | 3 | 16.6 | 0.0 |
| 5.5 | Anatolomys teilhardi | ER_Ate2 | 2 | -11.8 | 0.1 | -11.3 | 3 | 15.3 | 0.0 |
| 5.5 | Pseudomeriones abbreviatus | ER_Pab1 | 2 | -11.2 | 0.1 | -10.7 | 8 | 17.3 | 0.2 |
| 5.5 | Pseudomeriones abbreviatus | ER_Pab2 | 2 | -11.2 | 0.2 | -10.7 | 8 | 17.7 | 0.2 |
| 5.5 | Pseudomeriones abbreviatus | ER_Pab3 | 3 | -5 | 0.7 | -4.5 | 60 | 17.9 | 0.0 |
| 5.5 | Pseudomeriones abbreviatus | ER_Pab4 | 2 | -11.4 | 0.1 | -10.9 | 6 | 16.9 | 0.2 |
| 5.5 | Pseudomeriones abbreviatus | ER_Pab5 | 2 | -11.6 | 1.0 | -11.1 | 5 | 17.3 | 0.4 |
| 5.5 | Pseudomeriones abbreviatus | ER_Pab6 | 2 | -11.2 | 0.0 | -10.7 | 7 | 15.0 | 0.2 |
| 5.5 | Pseudomeriones abbreviatus | ER_Pab7 | 2 | -8.5 | 0.3 | -8 | 31 | 15.9 | 0.0 |
| 5.5 | Occitanomys pusillus | ER_Npu1 | 2 | -10.5 | 0.3 | -10 | 14 | 18.3 | 0.1 |
| 5.5 | Occitanomys pusillus | ER_Npu2 | 2 | -8.4 | 0.2 | -7.9 | 32 | 18.1 | 0.0 |
| 5.5 | Occitanomys pusillus | ER_Npu3 | 2 | -6.2 | 0.2 | -5.7 | 50 | 17.6 | 0.2 |
| 5.5 | Occitanomys pusillus | ER_Npu4 | 2 | -10.3 | 0.2 | -9.8 | 16 | 17.3 | 0.2 |
| 5.5 | Occitanomys pusillus | ER_Npu5 | 2 | -10.9 | 0.1 | -10.4 | 10 | 17.0 | 0.4 |
| 5.5 | Occitanomys pusillus | ER_Opu1 | 2 | -12.9 | 0.4 | -12.4 | 0 | 15.7 | 0.0 |
| 5.5 | Occitanomys pusillus | ER_Opu2 | 2 | -12 | 0.2 | -11.5 | 1 | 15.8 | 0.1 |
| 5.5 | Occitanomys pusillus | ER-Opu8 | 2 | -11.7 | 0.5 | -11.2 | 3 | 16.4 | 0.2 |
| 5.5 | Occitanomys pusillus | ER-Opu9 | 2 | -12.8 | 0.1 | -12.3 | 0 | 15.5 | 0.1 |
| 5.5 | Occitanomys pusillus | ER-Opu10 | 2 | -12.9 | 0.0 | -12.4 | 0 | 16.0 | 0.1 |
| 5.5 | Occitanomys pusillus | ER-Opu11 | 1 | -11.7 | | -11.2 | 4 | 20.1 | |
| 5.5 | Occitanomys pusillus | ER-Opu12 | 2 | -6.2 | 0.5 | -5.7 | 50 | 18.8 | 0.0 |
| 5.5 | Occitanomys pusillus | ER-Opu13 | 2 | -11 | 0.2 | -10.5 | 10 | 14.2 | 0.1 |
| 5.5 | Occitanomys pusillus | ER-Opu14 | 2 | -12 | 0.0 | -11.5 | 1 | 16.1 | 0.0 |
| 5.5 | Occitanomys pusillus | ER-Opu15 | 2 | -10.1 | 0.1 | -9.6 | 17 | 19.1 | 0.2 |
| 5.5 | Apodemus orientalis | ER_Aor1 | 2 | -6.6 | 0.2 | -6.1 | 47 | 16.3 | 0.0 |
| 5.5 | Apodemus orientalis | ER_Aor2 | 2 | -12.7 | 0.2 | -12.2 | 0 | 16.6 | 0.2 |
| 5.5 | Apodemus orientalis | ER_Aor3 | 3 | -5.6 | 0.2 | -5.1 | 55 | 17.9 | 0.1 |
| 5.5 | Apodemus orientalis | ER_Aor4 | 2 | -12.5 | 0.1 | -12 | 0 | 16.6 | 0.2 |
| 5.5 | Apodemus orientalis | ER_Aor5 | 2 | -10.7 | 0.3 | -10.2 | 12 | 15.9 | 0.0 |
| 5.5 | Apodemus orientalis | ER_Aor6 | 1 | -12.8 | | -12.3 | 0 | 15.3 | |
| 5.5 | Apodemus orientalis | ER_Aor7 | 2 | -12 | 0.1 | -11.5 | 1 | 16.0 | 0.2 |
| 5.5 | Orientalomys cf. similis | ER_Osi1 | 2 | -11.4 | 0.0 | -10.9 | 7 | 18.2 | 0.0 |
| 5.5 | Orientalomys cf. similis | ER_Osi2 | 1 | -12.6 | | -12.1 | 0 | 16.4 | |
| 5.5 | Orientalomys cf. similis | ER_Osi3 | 2 | -11.9 | 0.1 | -11.4 | 2 | 15.6 | 0.3 |
| 5.5 | Karnimata hipparionum | ER_Khi1 | 2 | -12.8 | 0.2 | -12.3 | 0 | 16.2 | 0.0 |
| 5.5 | Karnimata hipparionum | ER_Khi2 | 1 | -10.7 | | -10.2 | 12 | 17.8 | |

| | | | | | | | | | | |
|---|---|---|---|---|---|---|---|---|---|---|
| | 5.5 | Karnimata hipparionum | ER_Khi3 | 2 | -13.7 | 0.2 | -13.2 | 0 | 15.8 | 0.1 |
| | 5.5 | Karnimata hipparionum | ER_Khi4 | 2 | -10.7 | 0.1 | -10.2 | 12 | 17.6 | 0.1 |
| | 5.5 | Micromys chalceus | ER_Mch1 | 2 | -12.6 | 0.3 | -12.1 | 0 | 17.5 | 0.0 |
| | 5.5 | Micromys chalceus | ER-Mch1 | 2 | -12 | 0.2 | -11.5 | 1 | 16.3 | 0.2 |
| | 5.5 | Micromys chalceus | ER-Mch2 | 2 | -13.2 | 0.1 | -12.7 | 0 | 16.2 | 0.1 |
| | 5.5 | Micromys chalceus | ER-Mch3 | 1 | -13.3 | | -12.8 | 0 | 15.0 | |
| | 5.5 | Micromys chalceus | ER-Mch4 | 2 | -13.9 | 0.4 | -13.4 | 0 | 16.4 | 0.8 |
| | 5.5 | Eutemias ertemtensis | ER_Eer1 | 2 | -11.2 | 0.0 | -10.7 | 8 | 19.6 | 0.2 |
| | 5.5 | Eutemias ertemtensis | ER_Eer2 | 3 | -10.6 | 0.5 | -10.1 | 13 | 19.9 | 0.1 |
| | 5.5 | Eutemias ertemtensis | ER_Eer3 | 2 | -10.5 | 0.0 | -10 | 14 | 19.6 | 0.1 |
| | 5.5 | Eutemias ertemtensis | ER_Eer4 | 2 | -11.5 | 0.1 | -11 | 6 | 19.8 | 0.4 |
| | 5.5 | Eutemias ertemtensis | ER_Eer5 | 2 | -11.2 | 0.4 | -10.7 | 8 | 17.0 | 0.0 |
| | 5.5 | Eutemias ertemtensis | ER_Eer6 | 2 | -12.6 | 0.2 | -12.1 | 0 | 17.4 | 0.1 |
| | 5.5 | Eutemias ertemtensis | ER_Eer7 | 2 | -11.4 | 0.4 | -10.9 | 7 | 19.3 | 0.3 |
| | 5.5 | Eutemias ertemtensis | ER_Eer8 | 2 | -11.4 | 0.0 | -10.9 | 6 | 17.0 | 0.3 |
| | 5.5 | Sinotamias sp. | ER-Sin1 | 2 | -13.3 | 0.9 | -12.8 | 0 | 15.3 | 0.7 |
| | 5.5 | Prospermophilus sp. | ER-Psp1 | 2 | -10.9 | 0.6 | -10.4 | 11 | 15.6 | 0.3 |
| | 5.5 | Myomimus sinensis | ER_Msi1 | 1 | -12.2 | | -11.7 | 0 | 18.7 | |
| | 5.5 | Myomimus sinensis | ER_Msi2 | 2 | -11.6 | 0.1 | -11.1 | 5 | 17.6 | 0.1 |
| **Lingtai** | | | | | | | | | | |
| | 3.35 | Ochotona sp. | LIN_Ola1 | 4 | -10 | 0.2 | -9.5 | 18 | 15.9 | 0.2 |
| | 3.35 | Ochotona sp. | LIN_Ola2 | 3 | -10.5 | 0.1 | -10 | 14 | 14.2 | 0.1 |
| | 3.35 | Ochotona sp. | LIN_Ola3 | 4 | -12.4 | 0.2 | -11.9 | 0 | 14.1 | 0.7 |
| | 3.35 | Ochotona sp. | LIN_Ola4 | 4 | -10.1 | 0.5 | -9.6 | 18 | 15.8 | 0.3 |
| | 3.35 | Ochotona sp. | LIN_Ola5 | 8 | -9.1 | 0.5 | -8.6 | 26 | 17.8 | 0.5 |
| | 3.35 | Ochotona sp. | LI-OCH5 | 2 | -11.7 | 0.3 | -11.2 | 5 | 18.9 | 0.8 |
| | 3.35 | Ochotona sp. | LI-OCH6 | 2 | -10.6 | 0.3 | -10.1 | 14 | 15.4 | 0.1 |
| | 3.35 | Ochotona sp. | LI-OCH7 | 2 | -8.1 | 0.1 | -7.6 | 35 | 14.5 | 0.0 |
| | 3.35 | Ochotona sp. | LI-OCH8 | 2 | -10.1 | 0.2 | -9.6 | 18 | 15.1 | 0.1 |
| | 3.35 | Ochotona sp. | LI-OCH9 | 2 | -12 | 0.6 | -11.5 | 2 | 16.8 | 0.3 |
| | 3.35 | Ochotonoides complicidens | LI-OAM1 | 2 | -10.6 | 0.6 | -10.1 | 14 | 12.8 | 0.2 |
| | 3.35 | Ochotonoides complicidens | LI-OAM2 | 2 | -8.6 | 0.1 | -8.1 | 30 | 13.3 | 0.1 |
| | 3.35 | Ochotonoides complicidens | LI-OAM3 | 2 | -10.8 | 0.0 | -10.3 | 12 | 15.0 | 0.0 |
| | 3.35 | Ochotonoides complicidens | LI-OAM4 | 2 | -14.7 | 0.3 | -14.2 | 0 | 12.7 | 0.1 |
| | 3.16 | Ochotona sp. | LI-OCH1 | 3 | -11.4 | 0.7 | -10.9 | 7 | 16.7 | 0.7 |
| | 3.16 | Ochotona sp. | LI-OCH2 | 2 | -9.8 | 0.1 | -9.3 | 20 | 16.8 | 0.2 |
| | 3.16 | Ochotona sp. | LI-OCH3 | 2 | -11.1 | 0.2 | -10.6 | 9 | 16.0 | 0.0 |
| | 3.16 | Ochotona sp. | LI-OCH4 | 2 | -11.8 | 0.1 | -11.3 | 3 | 18.3 | 0.2 |
| | 3.35 | Prosiphneus licenti | LIN_Pro1 | 3 | -9.6 | 0.2 | -9.1 | 22 | 17.4 | 0.1 |
| | 3.35 | Prosiphneus licenti | LIN_Pro2 | 3 | -8.9 | 0.2 | -8.4 | 28 | 14.8 | 0.2 |
| | 3.35 | Prosiphneus licenti | LIN_Pro3 | 3 | -9.9 | 0.2 | -9.4 | 19 | 14.9 | 0.1 |
| | 3.35 | Mesosiphneus teilhardi | LI-MTE1 | 2 | -11 | 0.1 | -10.5 | 10 | 13.3 | 0.0 |

| | | | | | | | | | |
|---|---|---|---|---|---|---|---|---|---|
| 3.35 | Mesosiphneus teilhardi | LI-MTE2 | 3 | -11.7 | 0.5 | -11.2 | 5 | 14.3 | 0.4 |
| 3.35 | Mesosiphneus teilhardi | LI-MTE3 | 2 | -11.1 | 0.0 | -10.6 | 10 | 14.3 | 0.6 |
| 3.16 | Mesospihneus intermedius | LI-MIN1 | 2 | -11.6 | 0.2 | -11.1 | 5 | 15.8 | 0.5 |
| 3.16 | Mesospihneus intermedius | LI-MIN2 | 2 | -12.3 | 0.2 | -11.8 | 0 | 12.8 | 0.1 |
| 3.16 | Mesospihneus intermedius | LI-MIN3 | 2 | -11.7 | 0.1 | -11.2 | 4 | 11.2 | 0.3 |
| 3.16 | Mesospihneus intermedius | LI-MIN4 | 2 | -12.1 | 0.4 | -11.6 | 0 | 13.9 | 0.2 |
| 3.16 | Nannocricetus sp. | LI-NAN1 | 2 | -9 | 0.6 | -8.5 | 28 | 14.3 | 0.1 |
| 3.16 | Nannocricetus sp. | LI-NAN2 | 2 | -10.7 | 0.3 | -10.2 | 13 | 11.5 | 3.0 |
| 3.16 | Nannocricetus sp. | LI-NAN3 | 2 | -6.5 | 0.8 | -6 | 48 | 13.8 | 0.5 |
| 3.16 | Nannocricetus sp. | LI-NAN4 | 2 | -7.1 | 0.5 | -6.6 | 43 | 17.4 | 0.1 |
| 4.7 | Pseudomeriones abbreviatus | LI-PAB1 | 2 | -9.9 | 0.7 | -9.4 | 22 | 18.9 | 0.2 |
| 4.7 | Pseudomeriones abbreviatus | LI-PAB2 | 2 | -11 | 1.7 | -10.5 | 13 | 17.7 | 0.0 |
| 4.7 | Pseudomeriones abbreviatus | LI-PAB3 | 1 | -9.2 | | -8.7 | 28 | 16.1 | |
| 4.7 | Pseudomeriones abbreviatus | LI-PAB4 | 2 | -12.2 | 0.4 | -11.7 | 3 | 16.3 | 0.2 |
| 4.7 | Pseudomeriones abbreviatus | LI-PAB5 | 2 | -3.9 | 0.1 | -3.4 | 73 | 15.5 | 0.2 |
| 5.8 | Pseudomeriones abbreviatus | LI-PAB6 | 2 | -7.8 | 0.4 | -7.3 | 37 | 16.3 | 0.3 |
| 5.8 | Pseudomeriones abbreviatus | LI-PAB7 | 2 | -11.8 | 0.2 | -11.3 | 3 | 14.6 | 0.5 |
| 5.8 | Pseudomeriones abbreviatus | LI-PAB8 | 2 | -14 | 0.6 | -13.5 | 0 | 14.3 | 0.4 |
| 6.45 | Pseudomeriones abbreviatus | LI-PAB9 | 1 | -15.4 | | -14.9 | 0 | 16.2 | |
| 6.45 | Pseudomeriones abbreviatus | LI-PAB10 | 2 | -14.3 | 0.3 | -13.8 | 0 | 16.4 | 0.1 |
| 4.8 | Pseudomeriones abbreviatus | LI-PAB12 | 3 | -9.5 | 0.4 | -9 | 25 | 18.2 | 0.1 |
| 4.8 | Pseudomeriones abbreviatus | LI-PAB13 | 2 | -9.2 | 1.0 | -8.7 | 28 | 18.1 | 0.3 |
| 4.8 | Pseudomeriones abbreviatus | LI-PAB14 | 2 | -10.3 | 1.3 | -9.8 | 18 | 15.3 | 0.0 |
| 4.8 | Pseudomeriones abbreviatus | LI-PAB15 | 2 | -13.4 | 0.1 | -12.9 | 0 | 17.0 | 0.1 |
| 3.16 | Bahomys sp. | LI-BAH1 | 3 | -9.2 | 0.3 | -8.7 | 25 | 19.1 | 0.3 |
| 3.16 | Bahomys sp. | LI-BAH2 | 3 | -10.9 | 0.3 | -10.4 | 11 | 16.9 | 0.4 |
| 3.16 | Bahomys sp. | LI-BAH3 | 2 | -13.3 | 0.2 | -12.8 | 0 | 17.6 | 0.4 |
| 3.16 | Bahomys sp. | LI-BAH4 | 2 | -10.3 | 0.3 | -9.8 | 16 | 16.8 | 0.2 |
| 3.46 | Bahomys sp. | LI-BAH5 | 2 | -11 | 0.3 | -10.5 | 10 | 19.5 | 0.1 |
| 3.46 | Bahomys sp. | LI-BAH6 | 2 | -13.8 | 0.8 | -13.3 | 0 | 17.6 | 1.0 |
| 3.46 | Bahomys sp. | LI-BAH7 | 2 | -9.2 | 0.2 | -8.7 | 25 | 14.7 | 0.4 |
| 3.16 | Allocricetus bursae | LI-ABU1 | 2 | -10 | 0.1 | -9.5 | 19 | 16.2 | 0.3 |
| 3.16 | Allocricetus bursae | LI-ABU2 | 2 | -9.1 | 0.2 | -8.6 | 27 | 14.0 | 0.4 |
| 3.16 | Allocricetus bursae | LI-ABU3 | 2 | -10.5 | 0.3 | -10 | 14 | 16.0 | 0.1 |
| 3.16 | Allocricetus bursae | LI-ABU4 | 2 | -11.6 | 0.0 | -11.1 | 5 | 17.6 | 0.5 |
| 6.6 | Chardinomys primitivus | LI-CPR1 | 2 | -9.5 | 0.2 | -9 | 23 | 14.9 | 0.2 |
| 6.6 | Chardinomys primitivus | LI-CPR3 | 2 | -9.2 | 0.2 | -8.7 | 26 | 16.4 | 0.1 |

| | | | | | | | | | | |
|---|---|---|---|---|---|---|---|---|---|---|
| | 6.6 | Chardinomys primitivus | LI-CPR4 | 2 | -13.2 | 0.8 | -12.7 | 0 | 18.6 | 0.0 |
| | 6.6 | Karnimata hipparionum | LI-KHI1 | 3 | -9.6 | 0.5 | -9.1 | 22 | 16.4 | 0.3 |
| | 6.6 | Karnimata hipparionum | LI-KHI2 | 2 | -9.5 | 0.1 | -9 | 23 | 16.2 | 0.1 |
| | 6.6 | Karnimata hipparionum | LI-KHI3 | 2 | -13.6 | 0.0 | -13.1 | 0 | 17.3 | 0.3 |
| **Yanmou** | | | | | | | | | | |
| | 8 | Platacanthomys dianensis | YAN_Pdi1/2 | 2 | -13.1 | 0.2 | -12.6 | 0 | 15.3 | 0.15 |
| | 8 | Platacanthomys dianensis | YAN_Pdi3/4/5 | 3 | -12 | 0.1 | -11.5 | 1 | 16.5 | 0.52 |
| | 8 | Typhlomys primitivus | YAN_Tpr1 | 1 | -14 | | -13.5 | 0 | 15.8 | |
| | 8 | Typhlomys primitivus | YAN_Tpr2/3 | 2 | -13.3 | 0.2 | -12.8 | 0 | 15.7 | 0.7 |
| | 8 | Typhlomys primitivus | YAN_Tpr4 | 1 | -13.6 | | -13.1 | 0 | 14.2 | |
| | 8 | Linomys yunnanensis | YAN_Pyu1 | 1 | -14.5 | | -14 | 0 | 15.2 | |
| | 8 | Linomys yunnanensis | YAN_Pyu2 | 2 | -13.6 | 0.1 | -13.1 | 0 | 14.1 | 0.1 |
| | 8 | Linomys yunnanensis | YAN_Pyu3 | 2 | -11.3 | 0.1 | -10.8 | 7 | 16.3 | 0.1 |
| | 8 | Linomys yunnanensis | YAN_Pyu4 | 2 | -15.3 | 0.1 | -14.8 | 0 | 13.0 | 0.1 |
| **Lufeng** | | | | | | | | | | |
| | 7.5 | Linomys yunnanensis | LUF_Pyu1 | 1 | -13.5 | | -13 | 0 | 15.7 | |
| | 7.5 | Linomys yunnanensis | LUF_Pyu2 | 1 | -11.7 | | -11.2 | 3 | 15.1 | |
| | 7.5 | Linomys yunnanensis | LUF_Pyu4 | 2 | -14.7 | 0.6 | -14.2 | 0 | 14.4 | 0.3 |
| | 7.5 | Linomys yunnanensis | LUF_Pyu5 | 1 | -12.3 | | -11.8 | 0 | 16.9 | |
| | 7.5 | Linomys yunnanensis | LUF_Pyu6 | 2 | -9.4 | 0.3 | -8.9 | 23 | 17.3 | 0.1 |
| | 7.5 | Linomys yunnanensis | LUF_Pyu8 | 1 | -16.1 | | -15.6 | 0 | 15.9 | |
| | 7.5 | Kowalskia hanae | LUF_Kmo1 | 3 | -15 | 0.3 | -14.5 | 0 | 14.7 | 0.2 |
| | 7.5 | Kowalskia hanae | LUF_Kmo2 | 1 | -14.9 | | -14.4 | 0 | 15.9 | |
| | 7.5 | Kowalskia hanae | LUF_Kmo4 | 1 | -14 | | -13.5 | 0 | 14.9 | |

[a] number of analyses on a single tooth specimen
[b] laser-produced values were adjusted +0.5‰ for the offset between the laser method and conventional phosphoric acid method (Passey and Cerling, 2006)

**B) Carbon isotope values of large herbivore tooth enamel from Yanmou, Yunnan province (Xiaohe and Leilao localities) from Passey, 2007 [a].**

| Locality | Age (Ma)[b] | Taxon | sample ID | $\delta^{13}C^{c}$ | $\delta^{18}O^{c}$ | C4% |
|---|---|---|---|---|---|---|
| **Xiaohe** | | | | | | |
| | 8 | Rhinocerotidae | CN2006-YNM-013 | -14.6 | -11 | 0 |
| **Leilao** | | | | | | |
| | 8 | Hipparion | CN2006-YNM-032 | -12.1 | -11.2 | 0 |
| | 8 | Hipparion | CN2006-YNM-033 | -12.2 | -9.3 | 0 |
| | 8 | Rhinocerotidae | CN2006-YNM-034 | -10.6 | -12.4 | 0 |
| | 8 | Hipparion | CN2006-YNM-035 | -12.5 | -8.6 | 0 |

| | | | | | |
|---|---|---|---|---|---|
| 8 | Rhinocerotidae | CN2006-YNM-036 | -13.1 | -12.4 | 0 |
| 8 | | CN2006-YNM-037-out | -13.1 | -9.7 | 0 |
| 8 | Ursidae | CN2006-YNM-038 | -11.9 | -10.2 | 0 |
| 8 | Hipparion | CN2006-YNM-039 | -13.9 | -10 | 0 |
| 8 | Cervidae | CN2006-YNM-040 | -11.2 | -10.2 | 0 |
| 8 | Tragulidae | CN2006-YNM-041 | -9.1 | -7.1 | 0 |
| 8 | Cervidae | CN2006-YNM-042 | -10.8 | -14.9 | 0 |
| 8 | Cervidae | CN2006-YNM-043 | -10.8 | -4.8 | 0 |
| 8 | Cervidae | CN2006-YNM-044-out | -11.3 | -7.7 | 0 |

[a] Passey, B.H., 2007.Stable isotope paleoecology: methodological advances and applications to the Late Neogene environmental history of China. Dissertation, pp. 266, Department of Geology and Geophysics, The University of Utah.

[b] Age assignment in Passey (2007) is 7.5 Ma but was changed to match the age estimate for Yuanmou used in this paper.
[c] Isotope analyses were done following the conventional phosphoric acid digestion method.